Study on Functional Regulation of Iron Regulatory Proteins Mediated by Heme Binding to Heme Regulatory Motifs

（ヘム制御モチーフへのヘム結合を介した鉄制御蛋白質 **IRPs** の機能制御に関する研究）

Yudai Nishitani

西谷　雄大

Graduate School of Chemical Sciences and Engineering,

Hokkaido University

北海道大学大学院　総合化学院

2019

ACKNOWLEDGEMENTS

This thesis entitled "Study on Functional Regulation of Iron Regulatory Proteins Mediated by Heme Binding to Heme Regulatory Motifs" was supervised by Professor Koichiro Ishimori (Department of Chemistry, Faculty of Science, Hokkaido University). The work in this thesis has been conducted from April 2013 to March 2019.

First, I would like to express my great gratitude to Professor Koichiro Ishimori. He always gave me continuous guidance, fruitful discussion, and hearty encouragement.

I gratefully appreciate Dr. Takeshi Uchida (Hokkaido University) for his precise indication and technical assistance. I am also grateful to Dr. Hiroshi Takeuchi for his passionate inspiration, Dr. Tomohide Saio for his helpful discussion, and Secretary Maki Tanaka for accepting the troublesome office procedure. I also thank the past and current members of Structural Chemistry Laboratory for helps and assistances.

I was given a lot of cooperation with a number of researchers for conducting the researches. I appreciate Professor Kazuhiro Iwai and Dr. Yukiko Takeda (Kyoto University) for the construction of baculovirus to express IRPs. I also deeply appreciate Professor Iqbal Hmaza and Dr. Xiaojing Yuan (University of Maryland, Maryland, USA) for their kind acceptance about my stay there for one month between Oct. – Nov. 2017 and for two months between Jul. – Sep. 2018. I have learned a lot about the treatment of mammalian cell, protein expression and *in vivo* experiments involved in cellular heme trafficking.

At the review of this work, Professor Yota Murakami (Laboratory of Bioorganic Chemistry), Professor Masako Kato (Coordination Chemistry Laboratory), Professor Mutsumi Takagi (Laboratory of Cell Processing Engineering), Professor Yasuyuki Fujita (Division of Molecular Oncology), and Professor Takeshi Uchida (Structural Chemistry Laboratory) gave me the valuable suggestions and guidance.

I would also like to be grateful to Ambitious Leader's Program (ALP) in Hokkaido University. I have been belonging to this program since Oct. 2014. This program provided me the opportunities to visit abroad, learn the multidisciplinary concept as well as monthly financial support for daily life. I also thank Professors, staffs and students who belong to this program for their kind support and letting me learn and experience a lot outside of the laboratory.

Additionally, the "Organization of young researchers in Biochemistry", particularly that of Hokkaido branch, have gave me a lot of knowledges and concepts related to wide area of biochemistry and life sciences. I have also been able to experience a lot for organizing the group and planning events by discussions with the members.

Lastly, I would like to appreciate my family, Mr. Ryuhei Mogami, Mrs. Junko Mogami, Mrs. Mai Koga, with my whole heart. They have mentally and financially supported me a lot. I'm certain of spending unforgettable times and having invaluable experiences in Hokkaido University for nine years owing to their assistances.

September, 2019

Graduate School of Chemical Sciences and Engineering, Hokkaido University

Yudai Nishitani

LIST OF PUBLICATIONS

Chapter II

Yudai Nishitani, Hirotaka Okutani, Yukiko Takeda, Takeshi Uchida, Kazuhiro Iwai, and Koichiro Ishimori

"Specific Heme Binding to Heme Regulatory Motifs in Iron Regulatory Proteins and Its Functional Significance"

Journal of Inorganic Biochemistry, **198**, 110726 (2019)

Chapter III

Yudai Nishitani, Hirotaka Okutani, Yukiko Takeda, Takeshi Uchida, Kazuhiro Iwai, and Koichiro Ishimori

"Specific Heme Binding to Heme Regulatory Motifs in Iron Regulatory Proteins and Its Functional Significance"

Journal of Inorganic Biochemistry, **198**, 110726 (2019)

Chapter IV

Yudai Nishitani, Hirotaka Okutani, Yukiko Takeda, Takeshi Uchida, Kazuhiro Iwai, and Koichiro Ishimori

"Specific Heme Binding to Heme Regulatory Motifs in Iron Regulatory Proteins and Its Functional Significance"

Journal of Inorganic Biochemistry, **198**, 110726 (2019)

LIST OF PRESENTATIONS

Oral Presentations

1. Yudai Nishitani, Takeshi Uchida, Kazuhiro Iwai, and Koichiro Ishimori

   “Identification of structurally affected region in iron regulatory protein 2 upon its oxidative modification”

   The Meeting in Winter 2014 of the Hokkaido Branch of the Chemical Society of Japan (Sapporo, Japan) January 29, 2014

2. Yudai Nishitani, Yukiko Takeda, Takeshi Uchida, Kazuhiro Iwai, and Koichiro Ishimori

   “The mechanism for the heme-dependent oxidation for the functional regulation of iron regulatory protein 2”

   The Meeting in Summer 2014 of the Hokkaido Branch of the Chemical Society of Japan (Sapporo, Japan) July 12, 2014

3. Yudai Nishitani, Yukiko Takeda, Takeshi Uchida, Kazuhiro Iwai, and Koichiro Ishimori

   “Mechanism of Heme-dependent Oxidative Modification in Iron Regulatory Proteins 2 (IRP2)”

   Hokkaido University - University of Strasbourg Joint Workshop by Graduate Students (Sapporo, Japan) February 10, 2015

4. Yudai Nishitani, Yukiko Takeda, Takeshi Uchida, Kazuhiro Iwai, and Koichiro Ishimori

   “Mechanism of Oxidative Modification in Iron Regulatory Proteins 2 (IRP2) Mediated by Heme Binding as a Cellular Iron Signal”

1st Student Winter Workshop (Strasbourg, France) March 14, 2016

5. Yudai Nishitani, Yukiko Takeda, Takeshi Uchida, Kazuhiro Iwai, and Koichiro Ishimori

   "Mechanism of Oxidative Modification in Iron Regulatory Proteins 2 (IRP2) Mediated by Heme Binding as a Cellular Iron Signal"

   HU-JKU Joint Symposium on Chemical Sciences and Engineering (Linz, Austria) February 22, 2017

Poster Presentations

1. Yudai Nishitani, Yukiko Takeda, Takeshi Uchida, Kazuhiro Iwai, and Koichiro Ishimori

   "Functional regulation by heme-dependent oxidative modification in Iron Regulatory Protein 2 (IRP2)"

   The 24th Symposium on Role of Metals in Biological Reactions, Biology and Medicine (Kyoto, Japan) June 14-15, 2014

2. Yudai Nishitani, Yukiko Takeda, Takeshi Uchida, Kazuhiro Iwai, and Koichiro Ishimori

   "Mechanism of Heme-dependent Oxidative Modification in Iron Regulatory Protein 2 (IRP2)"

   The 87th Annual Meeting of the Japanese Biochemical Society, (Kyoto, Japan), October 15-18, 2014

3. Yudai Nishitani, Yukiko Takeda, Takeshi Uchida, Kazuhiro Iwai, and Koichiro Ishimori

“Mechanism of Heme-dependent Oxidative Modification in Iron Regulatory Protein 2 (IRP2)”

17th SNU-HU Joint Satellite Session (Sapporo, Japan) November 28-29, 2014

4. Yudai Nishitani, Yukiko Takeda, Takeshi Uchida, Kazuhiro Iwai, and Koichiro Ishimori

“Mechanism of Heme-dependent Oxidative Modification in Iron Regulatory Protein 2 (IRP2)”

2nd International Symposium on AMBITIOUS LEADER’ S PROGRAM (Sapporo, Japan) December 11, 2014

5. Yudai Nishitani, Yukiko Takeda, Takeshi Uchida, Kazuhiro Iwai, and Koichiro Ishimori

“Mechanism of Heme-dependent Oxidative Modification in Iron Regulatory Protein 2 (IRP2)”

‘Metals in Biology’ in Wako (Saitama, Japan) June 16, 2015

6. Yudai Nishitani, Yukiko Takeda, Takeshi Uchida, Kazuhiro Iwai, and Koichiro Ishimori

“Mechanism of Heme-dependent ROS generation and Oxidative Modification in Iron Regulatory Protein 2 (IRP2)”

3rd International Symposium on AMBITIOUS LEADER’ S PROGRAM (Sapporo, Japan) November 18, 2015

7. Yudai Nishitani, Yukiko Takeda, Takeshi Uchida, Kazuhiro Iwai, and Koichiro Ishimori

"Mechanisms of heme-mediated reactive oxygen species generation and oxidative modification of Iron Regulatory Protein 2"

The 90th Annual Meeting of the Japanese Biochemical Society, (Kobe, Japan), December 6-9, 2017

8. Yudai Nishitani, Yukiko Takeda, Takeshi Uchida, Kazuhiro Iwai, and Koichiro Ishimori

"Mechanisms of Heme-mediated Regulation of IRP2 Activity through Direct Heme Binding and Subsequent Oxidation in IRP2"

Gordon Research Conference, Chemistry and Biology of Tetrapyrroles, The Movement and Trafficking of Tetrapyrroles (Hemes, B12/Corrins, Bilins, and Chlorophyll) (Newport, USA) July 15-20, 2018

CONTENTS

CHAPTER I

GENERAL INTRODUCTIONS

Transition metals are pivotal in most of living organisms. Among the transition metals, iron is most abundant in our body and plays a crucial role for various biological reaction as a cofactor of the proteins. On the other hand, an excessive amounts of iron causes oxidative stress by reacting with molecular oxygen and generating reactive oxygen species (ROS) that induce the damage to nucleic acids and proteins. Therefore, the intracellular iron content must be strictly regulated. The general information for cellular iron metabolism including the function and physiological importance of iron regulatory proteins (IRPs) are described in this chapter.

1.1. Physiological Role of Iron

Iron is the second most abundant metal in the earth's crust and is also indispensable for living organisms. Its redox potential ranges from 1000 to −550 mV (*1*) enabling iron to readily accept or donate electrons that is essential for many important biological reactions such as electron transfer (*2*), oxygen transport (*3*) or DNA synthesis (*4*). Nearly 60% of total iron in body exists in red blood cells and iron deficiency in human body causes anemia (*1, 5*) . In contrast, iron is cytotoxic due to its high reactivity with molecular oxygen resulting in the generation of ROS that induce oxidative damage to biomolecules such as DNA, proteins and lipids (*6*). Iron accumulation in cells or tissues causes not only cirrhosis of liver and cancer (*7-9*), but is also correlated to some neurodegenerative diseases such as Alzheimer's disease or Parkinson's disease (*10, 11*). Therefore, maintaining homeostatic iron level in the cells and in the body is extremely important.

As there is no active mechanism to excrete iron from the body, absorption of dietary iron at the duodenum mucosa compensates nonspecific iron losses by cell desquamation

in the skin and intestine (*12, 13*). The absorbed iron is released from intestinal cells to plasma by an iron exporter, ferroportin, leading to increase of the body iron level. The iron regulatory hormone hepcidin regulates the iron level in body by controlling the amount of Ferroportin (*13-15*). Thus, the iron content in body is strictly regulated at duodenum mucosa.

1.2. Iron Uptake, Storage and Export in Mammalian Cell

The iron level in each cell is regulated as shown in Fig. 1.1 (*16, 17*). Iron released from intestinal cell is delivered to all tissues by an iron transporter transferrin (Tf) as Fe^{3+} in plasma. Most cells uptake the iron from plasma transferrin by receptor-mediated endocytosis and the iron-loaded transferrin and transferrin receptor (TfR) complex releases the iron within the endosome by a proton pump when the endosomal pH is acidic. The released iron is reduced to Fe^{2+} by the Six-Transmembrane Epithelial Antigen of Prostate-3 (STEAP3), and the Fe^{2+} is exported into the cytoplasm by the Divalent Metal Transport 1 (DMT1) protein. The exported iron presumably enters the cytosolic 'labile iron pool' (LIP) through chelation to reduce the cytotoxicity of iron (*18-20*). The cytosolic iron is utilized for biosynthesis of heme, iron-porphyrin complex, or iron-sulfur cluster at mitochondria (*21, 22*). Excess iron is either stored in ferritin (Ft) or exported out of the cell via ferroportin 1a (FPN1a). In this systematic regulation of iron homeostasis, the cellular iron level is regulated at the translational level by controlling the expression of TfR, Ft and FPN1a.

1.3. The IRPs/IRE System in Iron Homeostasis

In mammalian cells, iron regulatory proteins (IRPs) are known as the primary regulators for cellular iron metabolism by regulating the fate of the mRNA encoding TfR, Ft or FPN1a (Fig. 1.1) (*23-25*). There are two isomers of IRPs, IRP1 and IRP2, and their function in cellular iron metabolism are essentially the same. In iron-depleted cells, IRPs stably bind to a conserved stem-loop structural motif, called iron-responsive element (IRE), on the target mRNA. Consisting of about 30 nucleotides, IRE is an RNA hairpin containing highly conserved bulge C and a six-base loop sequence 5'-CAGUGX-3', where X can either be A, C or U but never G (Fig. 1.2) (*26*). IRE is found on the untranslated region (UTR) of the target mRNAs. On the mRNA of Ft or FPN1a, IRE is located on their 5' UTR and the binding of IRPs inhibits the translation initiation by ribosome, leading to the decrease in their expression (*27-29*). The IRE in the TfR mRNA is found on its 3' side and binding of IRPs protects the mRNA from endonucleolytic cleavage, resulting in stabilization of mRNA and increase in the expression of proteins (*30*).

Binding of IRPs to IRE alters protein expression; it represses iron storage by Ft and iron efflux via FPN1a, and enhances iron uptake through TfR consequently increasing iron bioavailability (Fig. 1.3). On the other hand, when iron is sufficient in cells, IRPs lacks the IRE binding activity in an iron/heme dependent manner. Therefore Ft and FPN1a are steadily expressed and the amount of TfR in an iron-replete cell is reduced, resulting in the decrease in iron bioavailability (Fig. 1.4). Taken together, IRPs strictly maintain the iron homeostasis via IRE binding to target mRNAs affecting expression of proteins involved in iron uptake and storage.

1.4. Structure, Function, and Physiological Importance of IRP1 and IRP2

IRP1 and IRP2 amino acid sequences share approximately 57% homology and 75% similarity (Fig. 1.5). Despite this, there are differences between IRP1 and IRP2 structure, function, and physiological role. IRP1 has 889 amino acid residues with a mass of about 98 kDa and consists of four structural domains (domain 1-4) including the linker between domain 3 and 4, as shown in the crystal structure with Ft mRNA (Figure 1.6a) (*31*). Under iron-replete conditions, IRP1 assembles with a [4Fe-4S] cluster at three cysteine residues, Cys437, Cys503 and Cys506, and functions as cytosolic aconitase (cAcn) that catalyzes conversion of citrate to isocitrate (*32*). The aconitase form of IRP1 lacks the IRE binding activity because of overlap of the active site for aconitase with the IRE binding site (Fig. 1.6b) (*33*). Therefore, IRP1 is a bifunctional protein switching its function through the association and dissociation of [4Fe-4S] cluster.

On the other hand, IRP2 has 963 amino acid residues with a mass of about 105 kDa. Although IRP2 is considered to be composed of four domains similar to IRP1, crystal structure of IRP2 has not yet been solved. Contrary to IRP1, IRP2 lacks the ability to assemble a [4Fe-4S] cluster. The binding of IRP2 to IRE is regulated by its degradation through the oxidation and ubiquitin-proteasome system under iron-replete conditions (*34, 35*). This degradation is supposed to be triggered by heme binding to IRP2 at the heme-regulated motif (HRM) located in the 73-amino-acid domain referred as Iron-Dependent degradation (IDD) domain that is absent in IRP1 (*36-38*). These facts demonstrate that under iron-sufficient conditions, while IRP1 loses the IRE binding activity by association of the [4Fe-4S] cluster, IRP2 suffers its degradation triggered by heme binding which functions as signal of cellular iron level (Fig. 1.7).

The difference in the ability of IRP1 and IRP2 to sense cellular iron level points to their different physiological importance. Genetic ablation of IRPs in mice indicated that IRP2 plays an important role in iron homeostasis (*39, 40*). This is because *IRP2*-knockout mice have developed a progressive neurodegenerative disease associated with the misregulation of iron metabolism in all tissues that express IRP2, whereas IRP1 knockout mice have showed the misregulation only in the tissues, in which the expression level of IRP1 greatly exceeds that of IRP2. It is then suggested that IRP2 is the major regulator of iron homeostasis and IRP1 mostly functions as cytosolic aconitase, and only a small fraction of IRP1 in the IRE-binding form contributes to the basal regulation of iron metabolism. On the other hand, both IRP1 and IRP2 can be targets of ubiquitination upon the interaction with SCF^{FBXL5} ubiquitin ligase complex, which directly senses non-heme iron and is stabilized by binding of iron and oxygen (*41-43*). Thus, both IRP1 and IRP2 are regulated via several pathways depending on iron and/or heme concentration in cells.

1.5. Heme-regulatory Motif (HRM) for Heme Sensing

As described above, heme-mediated regulation via heme binding to HRM in the IDD domain of IRP2 seems to be one of the dominant pathway for regulation of iron metabolism in mammalian cells. The HRM is a consensus sequence commonly consisting of Cys-Pro dipeptide, where the Cys residue serves as a ligand to ferric (Fe^{3+}) heme. This sequence is conserved among proteins regulated by reversible heme binding (*44, 45*). Proteins, which contain HRM and seem to be regulated by heme binding, perform a wide range of cellular functions. Examples include Rev-erbα and Rev-erbβ for circadian

rhythm (*46*), Bach1 for heme homeostasis (*47*), HRI for stress response (*48*) BK channel for ion channel (*49*) and p53 for tumor suppression (*50*). Because reversible heme binding to HRM regulates various physiological functions, the short sequence of HRM in IRP2 could have a potential as a ligand for heme.

A look at the sequence alignment of IRP1 and IRP2 (Fig. 1.5) shows the existence of two HRMs conserved between IRPs outside the IDD domain, raising the possibility that both IRPs could be regulated by heme binding to these HRM outside the IDD domain. Recent spectroscopic studies revealed that both IRP1 and IRP2 specifically bind to two and three molar equivalents of heme, respectively (*51*). Ligands for ferric heme was ascribed to both of Cys residue for five coordination and Cys/His residues for six-coordination, suggesting the heme ligation to Cys in each HRM.

While heme binding to IRP1 on the regulation of its function is not yet clear, heme binding to HRM in IDD domain is supposed to be important for induction of oxidation in IRP2 (*36*). Oxidized IRP2 is subsequently ubiquitinated by the E3 ubiquitin ligase, HOIL-1 (*52*). The molecular mechanism of this oxidation-induced ubiquitination is not yet known.

It is previously reported that the reduction of heme in IRP2 induces the replacement of ligand for heme from Cys201 to His204 (*36*) and leads to the formation of five-coordinate His-ligated ferrous heme intermediate (*51*), which is not formed in ferrous heme in IRP1. These findings indicate that the reduction of heme is responsible for oxidation in IRP2 and possibly the ferrous heme intermediate ligated with His204 is required for the generation of reactive oxygen species (ROS). In this thesis, I focused on the role of heme binding to each HRM in IRP1 and IRP2 including the effect on the

association with IRE and heme-mediated oxidation in IRP2.

In Chapter I, I observed the heme-induced inhibition of IRPs-IRE complex formation by performing native PAGE. The pre-treatment of heme to IRPs interfered the complex formation with IRE. In addition, the addition of heme to the pre-formed IRP2-IRE complex also exhibited the inhibition of their interaction, indicating that the heme bound to HRM in IDD domain promotes the dissociation of IRP2 from IRE. Given that the one of the HRM outside of IDD domain, which is conserved between IRP1 and IRP2, is placed near the IRE binding site, the heme binding to this HRM in IRPs could sterically inhibit the complex formation with IRE. On the other hand, the IDD domain is supposed not to relate the interaction with IRE, suggesting that the heme binding to HRM in the IDD domain may cause allosteric inhibition, which leads to the dissociation of IRP2 from IRE, probably owing to the heme-induced conformational changes in IRP2. Thus, I revealed that the heme binding to HRM in IRPs regulates the complex formation with IRE and their roles seem to be different on the heme-mediated regulation of IRPs.

In Chapter II, I investigated the *in vitro* heme-mediated oxidation in IRP2. The oxidation of amino acid residues in IRP2 was observed in the presence of heme and reductant, but not in IRP1 and IRP2 lacking IDD domain (IRP2ΔIDD). Therefore, it is clarified that the heme bound to IDD domain is responsible for the oxidation. As the catalase, the enzyme decomposing hydrogen peroxide (H_2O_2), suppressed the heme-mediated oxidation of IRP2, H_2O_2 is involved in the oxidation reaction. However, the reactivity of H_2O_2 is not enough to directly oxidize amino acid residues in IRP2, implying the further activation of H_2O_2 to more reactive species during the reaction. Since the metal chelator did not show the suppression of the oxidation of IRP2, and no degradation of heme seemed be involved in the oxidation, the activation of H_2O_2 requires the reaction

with heme-iron rather than non-heme iron, which is found in typical metal-catalyzed oxidation of proteins.

In Chapter IV, I found that the heme-iron in IRPs forms a high valent iron(IV)-oxo heme species in the presence of H_2O_2. Considering that the ·OH could be generated as the result of the formation of high valent heme-iron complex, I suspected that produced ·OH oxidized the amino acid in IRP2. To identify the oxidation site in IRP2, I obtained mass spectra for the peptide fragments and MS/MS spectra for amino acids fragments from the oxidized IRP2. As a result, I confirmed the oxidation at Met552 in domain 3 of IRP2. A model structure of IRP2 showed that Met552 is close to the IDD domain, indicating that the generated ·OH at heme-iron in the IDD domain could directly oxidize the Met552. Therefore, I proposed the mechanism for the heme-mediated oxidation of IRP2, which is triggered by the reduction of heme-iron in IRP2.

In Chapter V, based on the results and insights in Chapter II, III, IV, I discussed the whole mechanism for the regulation of IRPs mediated by the heme binding to their HRMs. The results in this thesis revealed that heme acts as a signaling molecule for maintaining cellular iron level by regulating the function of IRPs upon the binding to their HRMs. These findings provide a better understanding of the cellular iron metabolism which is complicated system and has been poorly understood, leading to contribute to new drug design or therapies for various kinds of diseases involved in the defect of cellular iron metabolism.

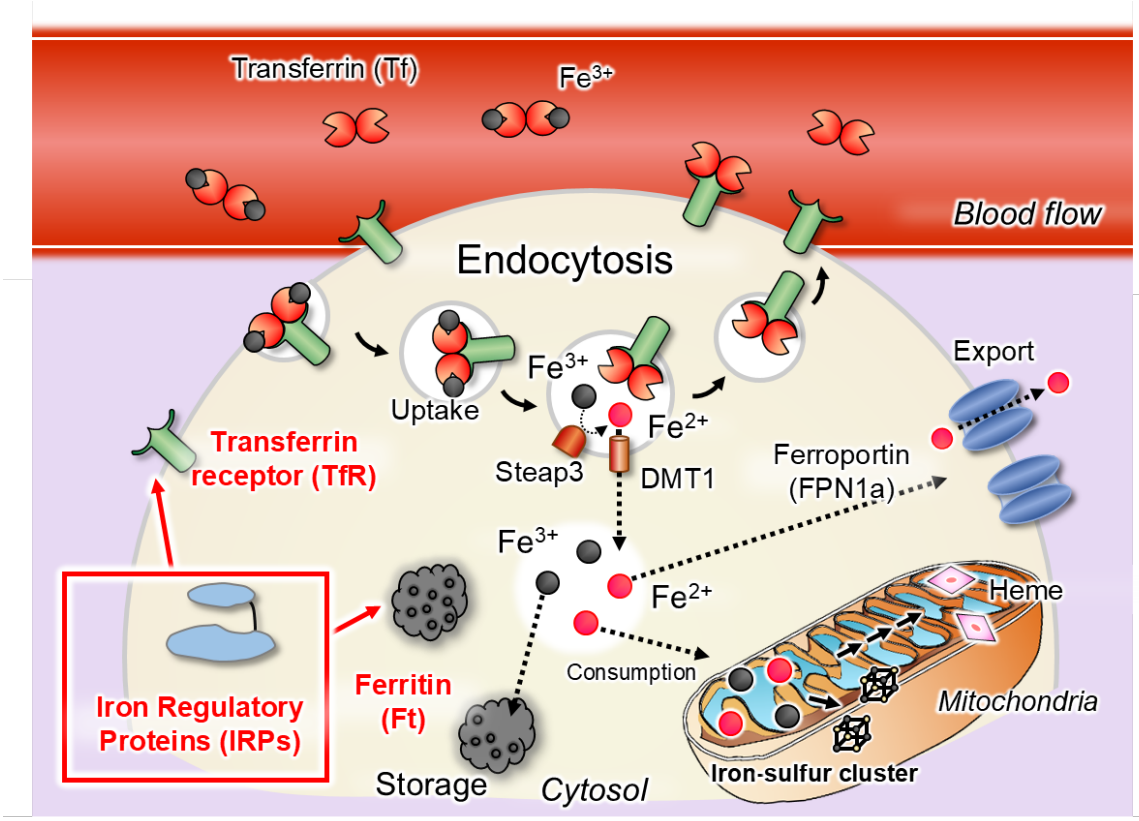

Figure 1.1. Iron metabolism in mammalian cell

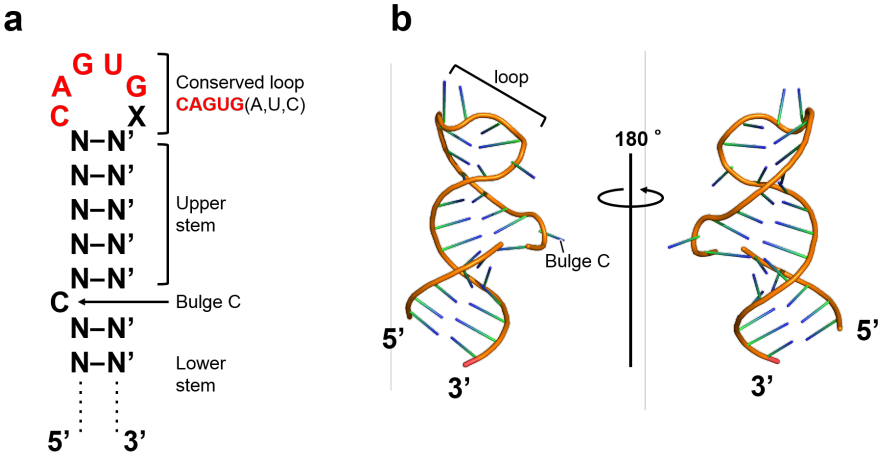

Figure 1.2. Structure of IRE

(a) Conserved IRE sequence and structural region. (b) 3D structure of IRE in Ft mRNA. (PDB ID: 3SNP)

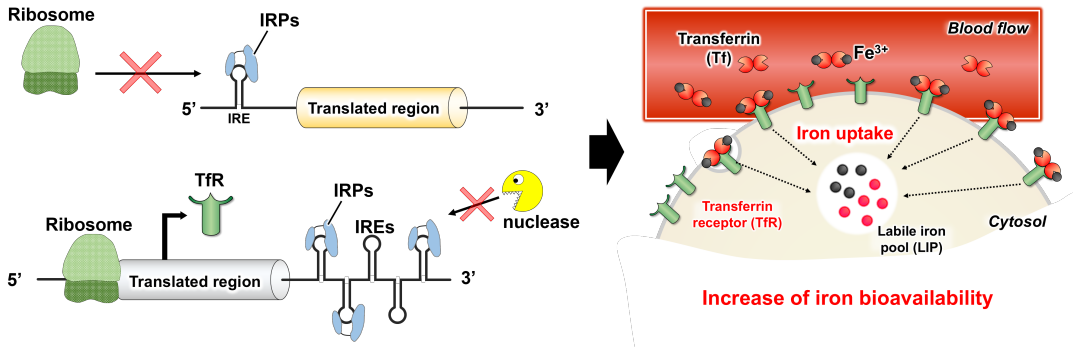

Figure 1.3. Regulation by IRPs in iron-deplete condition

In low iron condition, IRPs can stably bind to IRE. IRPs binding to IRE at 5' UTR inhibits the recognition and translation of the mRNA by ribosome, and the binding of IRPs to IRE at 3' UTR protects the mRNA from its cleavage by endonuclease, leading to the stable translation of TfR by ribosome.

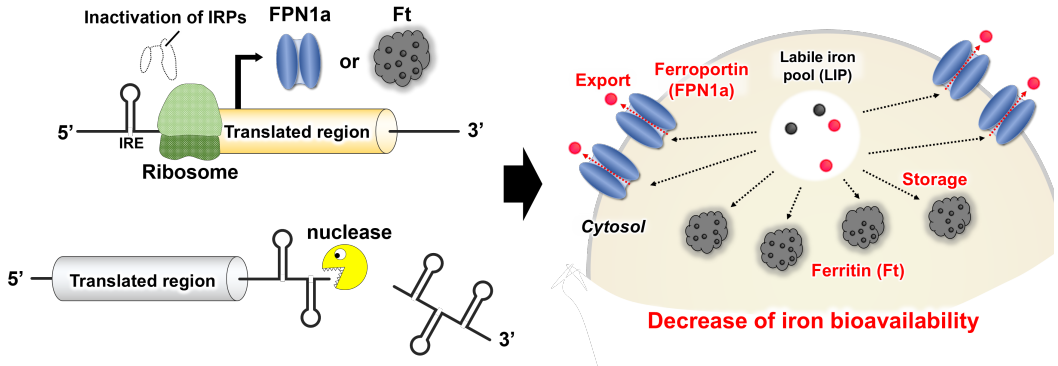

Figure 1.4. Regulation by IRPs in iron-replete condition

In high iron condition, IRPs lack the activity of binding to IRE so that ribosome stably translates the mRNA encoding FPN1a or Ft, and endnuclease destabilizes the mRNA which has IRE at 3' UTR, leading to the decrease of expression of the mRNA.

```
IRP1          MSNP-----FAHLAEPLDPVQPGKKFFNLNKLEDSRYGRLPFSIRVLLEAAIRNCDEFLV 55
IRP2          MDAPKAGYAFEYLIETLNDS-SHKKFFDVSKLG-TKYDVLPYSIRVLLEAAVRNCDGFLM 58
              *. *    * :* *.*:   . ****::.**  ::*. **:*********:**** **:
IRP1          KKQDIENILHWNVTQHKNIEVPFKPARVILQDFTGVPAVVDFAAMRDAVKKLGGDPEKIN 115
IRP2          KKEDVMNILDWKTKQS-NVEVPFFPARVLLQDFTGIPAMVDFAAMREAVKTLGGDPEKVH 117
              **:*: ***.*:..*  *:**** ****:******:**:*******:***.*******::
IRP1          PVCPADLVIDHSIQVDFNR---------------------------------------- 134
IRP2          PACPTDLTVDHSLQIDFSKCAIQNAPNPGGGDLQKAGKLSPLKVQPKKLPCRGQTTCRGS 177
              *.**:**.:***:*:**.:
IRP1          --------------------------------RADSLQKNQDLEFERNRERFEFLKWGSQ 162
IRP2          CDSGELGRNSGTFSSQIENTPILCPFHLQPVPEPETVLKNQEVEFGRNRERLQFFKWSSR 237
                                    ..::: ***::** *****::*:**.*:
IRP1          AFHNMRIIPPGSGIIHQVNLEYLARVVFDQDGYYYPDSLVGTDSHTTMIDGLGILGWGVG 222
IRP2          VLKNVAVIPPGTGMAHQINLEYLSRVVFEEKDLLFPDSVVGTDSHITMVNGLGILGWGVG 297
              .::*: :****:*: **:*****:****::..  :***:****** **::**********
IRP1          GIEAEAVMLGQPISMVLPQVIGYRLMGKPHPLVTSTDIVLTITKHLRQVGVVGKFVEFFG 282
IRP2          GIETEAVMLGLPVSLTLPEVVGCELTGSSNPFVTSIDVVLGITKHLRQVGVAGKFVEFFG 357
              ***:****** *:*:.**:*:* .* *..:*:*** *:** **********.********
IRP1          PGVAQLSIADRATIANMCPEYGATAAFFPVDEVSITYLVQTGRDEEKLKYIKKYLQAVGM 342
IRP2          SGVSQLSIVDRTTIANMCPEYGAILSFFPVDNVTLKHLEHTGFSKAKLESMETYLKAVKL 417
              .**:****.**:********** :*****:*::.:* :** .: **: ::.**:** :
IRP1          FRDFNDPSQDPDFTQVVELDLKTVVPCCSGPKRPQDKVAVSDMKKDFESCLGAKQGFKGF 402
IRP2          FRNDQNSSGEPEYSQVIQINLNSIVPSVSGPKRPQDRVAVTDMKSDFQACLNEKVGFKGF 477
              **: ::.* :*:::**::::*:::**. ********:***:***.**::**. * *****
IRP1          QVAPEHHNDHKTFIYDNTEFTLAHGSVVIAAITSCTNTSNPSVMLGAGLLAKKAVDAGLN 462
IRP2          QIAAEKQKDIVSIHYEGSEYKLSHGSVVIAAVISCTNNCNPSVMLAAGLLAKKAVEAGLR 537
              *:*.*:::*  :: *:.:*:.*:********: ****..******.*********:***.
IRP1          VMPYIKTSLSPGSGVVTYYLQESGVMPYLSQLGFDVVGYGCMTCIGNSGPLPEPVVEAIT 522
IRP2          VKPYIRTSLSPGSGMVTHYLSSSGVLPYLSKLGFEIVGYGCSTCVGNTAPLSDAVLNAVK 597
              * ***:********:**:**..***:****:***::***** **:**:.**.:.*::*:.
IRP1          QGDLVAVGVLSGNRNFEGRVHPNTRANYLASPPLVIAYAIAGTIRIDFEKEPLGVNAKGQ 582
IRP2          QGDLVTCGILSGNKNFEGRLCDCVRANYLASPPLVVAYAIAGTVNIDFQTEPLGTDPTGK 657
              *****: *:****:*****:   .**********:*******:.***:.****.:..*:
IRP1          QVFLKDIWPTRDEIQAVERQYVIPGMFKEVYQKIETVNESWNALATPSDKLFFWNSKSTY 642
IRP2          NIYLHDIWPSREEVHRVEEEHVILSMFKALKDKIEMGNKRWNSLEAPDSVLFPWDLKSTY 717
              :::*:****:*:*:: **.::** .*** : :***  *: **:* :*.. ** *: ****
```

```
IRP1          IKSPPFFENLTLDLQPPKSIVDAYVLLNLGDSVTTDHISPAGNIARNSPAARYLTNRGLT 702
IRP2          IRCPSFFDKLTKEPIALQAIENAHVLLYLGDSVTTDHISPAGSIARNSAAAKYLTNRGLT 777
              *:.*.**::** :  . ::* :*:*** **************.*****.**:******** 
IRP1          PREFNSYGSRRGNDAVMARGTFANIRLLNRFLNKQAPQTIHLPSGEILDVFDAAERYQQA 762
IRP2          PREFNSYGARRGNDAVMTRGTFANIKLFNKFIGKPAPKTIHFPSGQTLDVFEAAELYQKE 837
              ********:********:*******:*:*:*:.* **:***:***: ****:*** **: 
IRP1          GLPLIVLAGKEYGAGSSRDWAAKGPFLLGIKAVLAESYERIHRSNLVGMGVIPLEYLPGE 822
IRP2          GIPLIILAGKKYGSGNSRDWAAKGPYLLGVKAVLAESYEKIHKDHLIGIGIAPLQFLPGE 897
              *:***:****:**:*.*********:***:*********:**:.:*:*:*: **::****  
IRP1          NADALGLTGQERYTIIIPENLKPQMKVQVKLDTGKTFQAVMRFDTDVELTYFLNGGILNY 882
IRP2          NADSLGLSGRETFSLTFPEELSPGITLNIQTSTGKVFSVIASFEDDVEITLYKHGGLLNF 957
              ***:***:*:* ::: :**:*.* :.:::: .***.*..:  *: ***:* : :**:**:  
IRP1          MIRKMAK 889
IRP2          VARKFS- 963
              : **::
```

Figure 1.5. Sequence alignment of IRP1 and IRP2

IRP1 has 889 amino acid residues and its mass is 98,399 Da, while IRP2 has 963 amino acid residues and the mass is 105,012 Da. The IDD domain, ^{137}Cys-^{209}Pro, and heme-regulatory motif (HRM) in IRP2 are highlighted as red and bold with underline, respectively. ‘ * ’ means corresponding residues, ‘ : ’ means conserved residues, and ‘ . ’ means similar residues in the alignment.

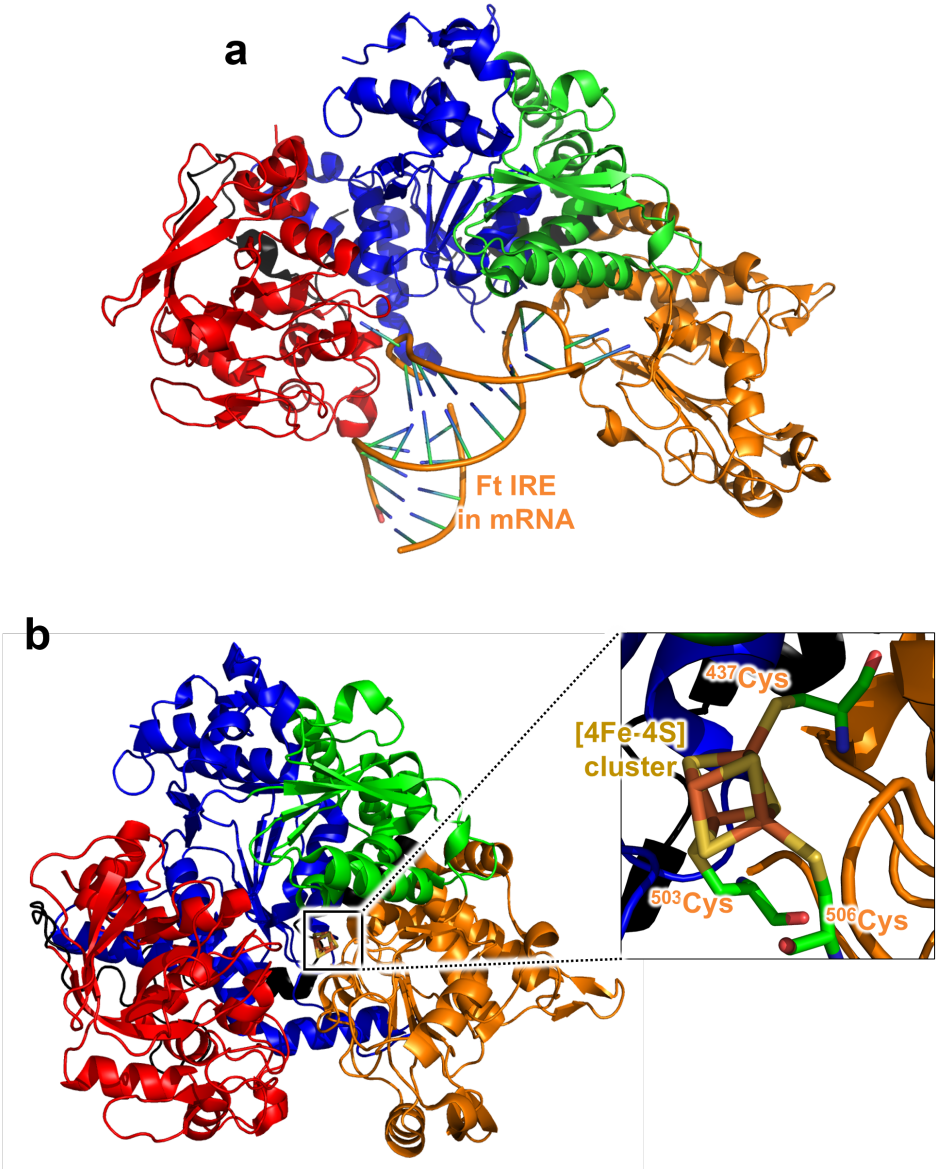

Figure 1.6. Crystal structures of two forms of IRP1

(a) Crystal structure of IRP1 with Ft IRE (PDB ID: 3SNP). (b) Crystal structure of IRP1 as the aconitase form with [4Fe-4S] cluster at the three cysteine residues in domain 3 (PDB ID: 2B3Y). Both structures show the domain 1 (blue), domain 2 (green), domain 3 (orange), linker (black), and domain 4 (red).

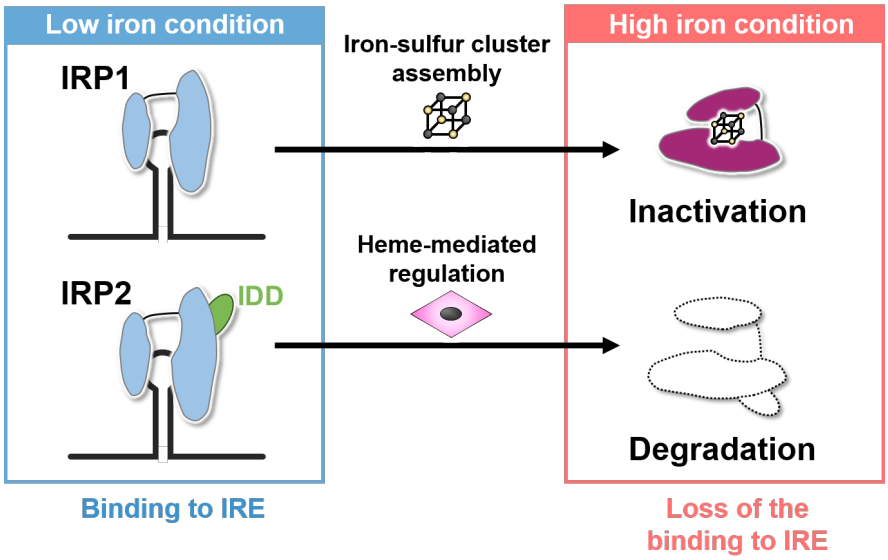

Figure 1.7. Mechanism of iron-dependent regulation of IRP1 and IRP2

In low-iron condition, IRPs stably bind to target IRE, while IRPs lack the IRE binding activity via different pathway in the iron-sufficient condition. IRP1 gains the aconitase activity by [4Fe-4S] cluster assembly, resulting the loss of the IRE binding, whereas IRP2 is regulated through the heme-mediated degradation.

References

1. K. Pantopoulos, S. K. Porwal, A. Tartakoff, L. Devireddy, Mechanisms of mammalian iron homeostasis. *Biochemistry* **51**, 5705-5724 (2012).
2. V. R. Kaila, M. I. Verkhovsky, M. Wikstrom, Proton-coupled electron transfer in cytochrome oxidase. *Chem Rev* **110**, 7062-7081 (2010).
3. J. A. Lukin, C. Ho, The structure--function relationship of hemoglobin in solution at atomic resolution. *Chem Rev* **104**, 1219-1230 (2004).
4. M. F. White, M. S. Dillingham, Iron-sulphur clusters in nucleic acid processing enzymes. *Curr Opin Struct Biol* **22**, 94-100 (2012).
5. N. C. Andrews, Disorders of iron metabolism. *N Engl J Med* **341**, 1986-1995 (1999).
6. R. Meneghini, Iron homeostasis, oxidative stress, and DNA damage. *Free Radic Biol Med* **23**, 783-792 (1997).
7. S. V. Torti, F. M. Torti, Iron and cancer: more ore to be mined. *Nature Reviews Cancer* **13**, 342-355 (2013).
8. J. A. Imlay, S. M. Chin, S. Linn, Toxic DNA Damage by Hydrogen-Peroxide through the Fenton Reaction Invivo and Invitro. *Science* **240**, 640-642 (1988).
9. M. Munoz, J. A. Garcia-Erce, A. F. Remacha, Disorders of iron metabolism. Part II: iron deficiency and iron overload. *J Clin Pathol* **64**, 287-296 (2011).
10. C. Quintana *et al.*, Study of the localization of iron, ferritin, and hemosiderin in Alzheimer's disease hippocampus by analytical microscopy at the subcellular level. *J Struct Biol* **153**, 42-54 (2006).
11. T. A. Rouault, Iron metabolism in the CNS: implications for neurodegenerative diseases. *Nat Rev Neurosci* **14**, 551-564 (2013).
12. B. J. Crielaard, T. Lammers, S. Rivella, Targeting iron metabolism in drug discovery and delivery. *Nat Rev Drug Discov* **16**, 400-423 (2017).
13. M. W. Hentze, M. U. Muckenthaler, B. Galy, C. Camaschella, Two to tango: regulation of Mammalian iron metabolism. *Cell* **142**, 24-38 (2010).
14. J. L. Babitt *et al.*, Bone morphogenetic protein signaling by hemojuvelin regulates hepcidin expression. *Nat Genet* **38**, 531-539 (2006).
15. E. Nemeth *et al.*, Hepcidin regulates cellular iron efflux by binding to ferroportin and inducing its internalization. *Science* **306**, 2090-2093 (2004).
16. M. U. Muckenthaler, S. Rivella, M. W. Hentze, B. Galy, A Red Carpet for Iron Metabolism. *Cell* **168**, 344-361 (2017).
17. P. Ponka, Cellular iron metabolism. *Kidney Int Suppl* **69**, S2-11 (1999).

18. O. Kakhlon, Z. I. Cabantchik, The labile iron pool: characterization, measurement, and participation in cellular processes(1). *Free Radic Biol Med* **33**, 1037-1046 (2002).
19. A. T. Aron, M. O. Loehr, J. Bogena, C. J. Chang, An Endoperoxide Reactivity-Based FRET Probe for Ratiometric Fluorescence Imaging of Labile Iron Pools in Living Cells. *J Am Chem Soc* **138**, 14338-14346 (2016).
20. B. Spangler *et al.*, A reactivity-based probe of the intracellular labile ferrous iron pool. *Nat Chem Biol* **12**, 680-685 (2016).
21. I. Hamza, H. A. Dailey, One ring to rule them all: Trafficking of heme and heme synthesis intermediates in the metazoans. *Bba-Mol Cell Res* **1823**, 1617-1632 (2012).
22. D. P. Barupala, S. P. Dzul, P. J. Riggs-Gelasco, T. L. Stemmler, Synthesis, delivery and regulation of eukaryotic heme and Fe-S cluster cofactors. *Arch Biochem Biophys* **592**, 60-75 (2016).
23. L. C. Kuhn, Iron regulatory proteins and their role in controlling iron metabolism. *Metallomics* **7**, 232-243 (2015).
24. K. Pantopoulos, Iron metabolism and the IRE/IRP regulatory system: an update. *Ann N Y Acad Sci* **1012**, 1-13 (2004).
25. R. S. Eisenstein, Iron regulatory proteins and the molecular control of mammalian iron metabolism. *Annu Rev Nutr* **20**, 627-662 (2000).
26. K. J. Addess, J. P. Basilion, R. D. Klausner, T. A. Rouault, A. Pardi, Structure and dynamics of the iron responsive element RNA: implications for binding of the RNA by iron regulatory binding proteins. *J Mol Biol* **274**, 72-83 (1997).
27. M. W. Hentze *et al.*, A Cis-Acting Element Is Necessary and Sufficient for Translational Regulation of Human Ferritin Expression in Response to Iron. *P Natl Acad Sci USA* **84**, 6730-6734 (1987).
28. N. K. Gray, M. W. Hentze, Iron regulatory protein prevents binding of the 43S translation pre-initiation complex to ferritin and eALAS mRNAs. *EMBO J* **13**, 3882-3891 (1994).
29. A. T. McKie *et al.*, A novel duodenal iron-regulated transporter, IREG1, implicated in the basolateral transfer of iron to the circulation. *Mol Cell* **5**, 299-309 (2000).
30. E. W. Mullner, L. C. Kuhn, A stem-loop in the 3' untranslated region mediates iron-dependent regulation of transferrin receptor mRNA stability in the cytoplasm. *Cell* **53**, 815-825 (1988).
31. W. E. Walden *et al.*, Structure of dual function iron regulatory protein 1 complexed

with ferritin IRE-RNA. *Science* **314**, 1903-1908 (2006).

32. E. Paraskeva, M. W. Hentze, Iron-sulphur clusters as genetic regulatory switches: The bifunctional iron regulatory protein-1. *Febs Letters* **389**, 40-43 (1996).
33. J. Dupuy *et al.*, Crystal structure of human iron regulatory protein 1 as cytosolic aconitase. *Structure* **14**, 129-139 (2006).
34. K. Iwai, R. D. Klausner, T. A. Rouault, Requirements for Iron-Regulated Degradation of the Rna-Binding Protein, Iron Regulatory Protein-2. *Embo Journal* **14**, 5350-5357 (1995).
35. F. Samaniego, J. Chin, K. Iwai, T. A. Rouault, R. D. Klausner, Molecular characterization of a second iron-responsive element binding protein, iron regulatory protein 2. Structure, function, and post-translational regulation. *J Biol Chem* **269**, 30904-30910 (1994).
36. H. Ishikawa *et al.*, Involvement of heme regulatory motif in heme-mediated ubiquitination and degradation of IRP2. *Mol Cell* **19**, 171-181 (2005).
37. J. Jeong, T. A. Rouault, R. L. Levine, Identification of a heme-sensing domain in iron regulatory protein 2. *J Biol Chem* **279**, 45450-45454 (2004).
38. L. S. Goessling, D. P. Mascotti, R. E. Thach, Involvement of heme in the degradation of iron-regulatory protein 2. *J Biol Chem* **273**, 12555-12557 (1998).
39. T. LaVaute *et al.*, Targeted deletion of the gene encoding iron regulatory protein-2 causes misregulation of iron metabolism and neurodegenerative disease in mice. *Nat Genet* **27**, 209-214 (2001).
40. E. G. Meyron-Holtz *et al.*, Genetic ablations of iron regulatory proteins 1 and 2 reveal why iron regulatory protein 2 dominates iron homeostasis. *EMBO J* **23**, 386-395 (2004).
41. A. A. Vashisht *et al.*, Control of iron homeostasis by an iron-regulated ubiquitin ligase. *Science* **326**, 718-721 (2009).
42. A. A. Salahudeen *et al.*, An E3 Ligase Possessing an Iron-Responsive Hemerythrin Domain Is a Regulator of Iron Homeostasis. *Science* **326**, 722-726 (2009).
43. K. Iwai, Regulation of cellular iron metabolism: Iron-dependent degradation of IRP by SCF(FBXL5) ubiquitin ligase. *Free Radic Biol Med*, (2018).
44. L. Zhang, L. Guarente, Heme Binds to a Short Sequence That Serves a Regulatory Function in Diverse Proteins. *Embo Journal* **14**, 313-320 (1995).
45. H. M. Girvan, A. W. Munro, Heme sensor proteins. *J Biol Chem* **288**, 13194-13203 (2013).
46. S. Raghuram *et al.*, Identification of heme as the ligand for the orphan nuclear

receptors REV-ERB alpha and REV-ERB beta. *Nat Struct Mol Biol* **14**, 1207-1213 (2007).

47. K. Ogawa *et al.*, Heme mediates derepression of Maf recognition element through direct binding to transcription repressor Bach1. *Embo Journal* **20**, 2835-2843 (2001).
48. J. Igarashi *et al.*, Elucidation of the heme binding site of heme-regulated eukaryotic initiation factor 2 alpha kinase and the role of the regulatory motif in heme sensing by spectroscopic and catalytic studies of mutant proteins. *Journal of Biological Chemistry* **283**, 18782-18791 (2008).
49. X. D. Tang *et al.*, Haem can bind to and inhibit mammalian calcium-dependent Slo1 BK channels. *Nature* **425**, 531-535 (2003).
50. J. Shen *et al.*, Iron Metabolism Regulates p53 Signaling through Direct Heme-p53 Interaction and Modulation of p53 Localization, Stability, and Function. *Cell Reports* **7**, 180-193 (2014).
51. M. Ogura *et al.*, Redox-dependent axial ligand replacement and its functional significance in heme-bound iron regulatory proteins. *J Inorg Biochem* **182**, 238-248 (2018).
52. K. Yamanaka *et al.*, Identification of the ubiquitin-protein ligase that recognizes oxidized IRP2. *Nat Cell Biol* **5**, 336-340 (2003).

CHAPTER II

HEME-INDUCED REGULATION OF COMPLEX FORMATION BETWEEN IRON REGULATORY PROTEINS AND ITS TARGET mRNA

ABSTRACT

Two homologs of iron regulatory proteins (IRPs), IRP1 and IRP2, are main regulators for iron metabolism in mammalian cells. IRPs associate with IRE to control the fate of target mRNA depending on cellular iron level. Although both IRPs conserve the heme regulatory motifs (HRM), only IRP2 has been thought to be regulated by heme binding to HRM in its iron-dependent degradation (IDD) domain that is not found in IRP1. In this chapter, to investigate the functional importance of heme binding on IRPs-IRE complex formation, I performed native PAGE assay. Following the clear detection of IRPs-IRE complex distinguishable from free IRPs, I demonstrated that the complex formation of both IRPs with IRE is inhibited upon heme binding to their HRM. Although heme can not bind to HRMs in the IRP1-IRE complex, the HRM in the IDD domain binds heme after the complex formation with IRE, resulting in dissociation of IRP2 from IRE. Since one of HRMs conserved between IRP1 and IRP2 is neighboring the amino acid that interacts with IRE based on the crystal structure of IRP1, heme binding to HRM near the IRE binding site sterically inhibits the complex formation. On the other hand, the HRM in the IDD domain is not overlapped by the IRE binding site, suggesting that the heme binding to HRM in the IDD domain non-competitively induces the dissociation of IRP2 from IRE. Thus, I revealed that the association of both IRPs and IRE are regulated by heme binding to HRMs, whereas the heme-induced dissociation of IRP2 via heme binding to HRM in the IDD domain functionally differentiates IRP2 from IRP1.

2.1. Introduction.

As described in chapter I, amino acid sequences of IRP1 and IRP2 share significant homology and conserve the IRE binding sites. Although both IRPs lose the IRE binding activity in an iron-replete condition and contain the conserved HRMs consisting of Cys-Pro dipeptide at corresponding amino acids, only IRP2 is known to be regulated by heme binding to HRM (*1-3*). The HRM (also known as CP motif) are found in various proteins that are functionally regulated by reversible heme binding (*4-8*). In the heme-mediated regulation of IRP2, binding of heme to HRM in the IDD domain triggers ubiquitination and degradation of IRP2, probably via oxidation of IRP2, consequently losing the IRE binding activity (*1, 3, 9*). In addition to heme binding to the IDD domain of IRP2, heme binding to HRMs in IRP1 was also proved by our recent study (*10, 11*). These studies reveal that heme specifically binds to all of HRMs in IRP1 and IRP2, suggesting that the regulation of IRPs by binding of heme at HRMs in IRP1 and HRMs outside of the IDD domain in IRP2. However, the functional importance of the heme binding to HRMs in IRP1 and HRMs outside of the IDD domain in IRP2 has not been clarified.

In this chapter, I revealed the heme-induced inhibition of the IRP2-IRE complex formation by using native PAGE. While heme binding to HRMs in both IRPs regulates the complex formation, only the HRM in IDD of IRP2 domain can bind to heme after the association of IRPs with IRE. I therefore discussed the different role of HRMs upon heme binding in the function of both IRPs.

2.2. Experimental Procedures.

2.2.1 Materials.

All chemicals were purchased from Wako Pure Chemical Industries (Osaka, Japan), Nacalai Tesque (Kyoto, Japan) or Sigma-Aldrich (St. Louis, MO, USA), and used without further purification.

2.2.2 Protein Expression and Purification

Procedures for the protein expression and purification were described by our previous paper (*10*). Briefly, His_6-tagged IRPs were expressed in High Five cells. The cells were then harvested and suspended in lysis buffer containing 50 mM Tris-HCl /100 mM NaCl (pH 7.4), 0.2 mg/mL heat-treated ribonuclease A (Roche Diagnosis, Basel, Switzerland) and 1 tablet/50 mL protease inhibitor cocktail tablet (Complete EDTA-free, Roche Diagnosis). Cells were homogenized and the supernatant were applied to Ni-NTA agarose resin (QIAGEN, Hilden, Germany). After the elution of IRPs from Ni-NTA resin, the eluate was applied to a HiLoad 16/600 Superdex 200 pg gel-filtration column (GE Healthcare, Uppsala, Sweden) pre-equilibrated with 50 mM HEPES-NaOH/100 mM NaCl (pH 7.4) for gel filtration chromatography. The protein concentrations of IRPs were determined using the absorbance at 280 nm with extinction coefficients (ε_{280}) of 84,690 (for IRP1) and 77,240 M^{-1} cm^{-1} (for IRP2), respectively, calculated in ProtParam (http://web.expasy.org/protparam/).

2.2.2 Native-PAGE Assay for Detection of IRPs-IRE Complex Formation

Human ferritin H chain IRE (5’-UUC CUG CUU CAA CAG UGC UUG GAC GGA A-3’) and IRE (-) (5’-UUC CUG CUU CAA CAG UGC UUG GAU GGA A-3’) were purchased from Eurofins Genomics as salt-free grade. This IRE was dissolved in 50 mM HEPES-

NaOH/100 mM NaCl (pH 7.4). After dissolving in the buffer, IRE was annealed by heating to 94 °C for 3 min with slow cooling to 25 °C over 6 hours in a water bath. To prepare the samples for native PAGE, hemin and/or IRE at different molar equivalents were added to 5 μM of purified IRPs. All sample were incubated for 15 min on ice to stabilize the complex with IRPs every time after the addition of heme and IRE. Each sample was mixed with the 5x gel loading buffer containing 315.5 mM Tris-HCl (pH 8.8), 40 % glycerol and 0.05% bromophenol blue and 15 μl of samples were applied to each well of 7.5 % (w/v) e-PAGEL polyacrylamide gels (Atto). Running gel with the constant current at 5 mA at 4 °C for 120 min was followed by the staining gels with Coomassie Brilliant Blue (Kanto Chemical). Gel images were obtained by scanning the gel and analyzed by using ImageJ and band intensities of the total proteins and the IRPs-IRE complexes (holo) in each lane were measured. The relative band intensities were normalized to the holo band intensity of IRPs with five equivalent IRE complex.

2.2.3 Confirmation of Secondary Structure of IRPs by CD Spectroscopy.

Purified IRPs were diluted to 2 μM in 50 mM Tris-HCl/100 mM NaCl (pH 7.4) to measure CD spectra. Heme solution for the CD measurements was prepared by dissolving hemin in 0.1 M NaOH and its concentration was determined from the absorbance at 385 nm using an extinction coefficient (ε_{385}) of 58.44 $mM^{-1}cm^{-1}$ (*12*). CD spectra in the far-UV region were measured with a J-1500 CD spectrometer (Jasco) over the spectral range of 190−250 nm at room temperature. Spectra were acquired at 0.2 nm intervals with a scan rate of 50 nm/min using a cylindrical quartz cuvette with a path length of 1 mm. The spectra were integrated by 10-times scanning and the buffer spectrum was subtracted from spectra for IRPs to obtain the actual sample spectra.

2.3. Results

2.3.1. Detection of IRPs-IRE Complex in native PAGE.

In the previous study, heme binding to HRMs in IRP1 and IRP2 was confirmed by spectroscopic heme titration combined with the site-directed mutagenesis of each HRMs in IRPs (*11*). However, the functional significances of the heme binding to HRMs in IRP1 and HRMs outside of the IDD domain in IRP2 are not revealed. Here, to clarify the effect of heme binding to IRPs for the complex formation with IRE, we performed native PAGE assay by which protein-nucleic acid complex formation is easily detectable (*13*).

Firstly, to confirm the detection of IRPs-IRE complex, we performed native PAGE of WT IRP1, WT IRP2 and IRP2ΔIDD with IRE RNA of human ferritin H chain (as illustrated in Fig. 1.2) and its point mutant (IRE (-)) with substitution of cytosine, which involves in the interaction with IRP1 (*14*), to uracil, which shows a much lower affinity for IRPs (*15*). The WT IRP2 were loaded with/without IRE including the IRE (-) and the images of CBB-stained gels were obtained after running (Fig. 2.1A and B). Fig. 2.1B clearly showed that WT IRP2 loaded with IRE exhibits upper broad bands and lower sharp bands, whereas the only upper bands appeared for free WT IRP2. The addition of IRE (-) with WT IRP2 showed only tiny lower band (Fig. 2.1A and C), demonstrating that the lower bands are specifically derived from IRPs-IRE complex. The IRPs-IRE complex were distinguishable from free IRPs because IRPs-IRE complex moves faster than the free IRPs owing to the negative charge of IRE. I also run a gel of the WT IRP1 and IRP2ΔIDD with/without IRE (Fig. 2.1D and E). Both of WT IRP1 and IRP2ΔIDD also form complex with IRE (Fig. 2.1D and E) like WT IRP2. The relative intensities of the bands derived from IRPs-IRE complex measured by using Image J were shown in Fig. 2.1C and F. As the intensity of the band for the IRPs-IRE complex with the three equivalents of IRE are similar to that with five equivalents of IRE for all construct of IRPs (Fig. 2.1F), IRPs seem to be almost saturated for the complex with IRE in the presence of five

equivalents of IRE. Thus, we could successfully detect the IRPs-IRE complex formation using native PAGE.

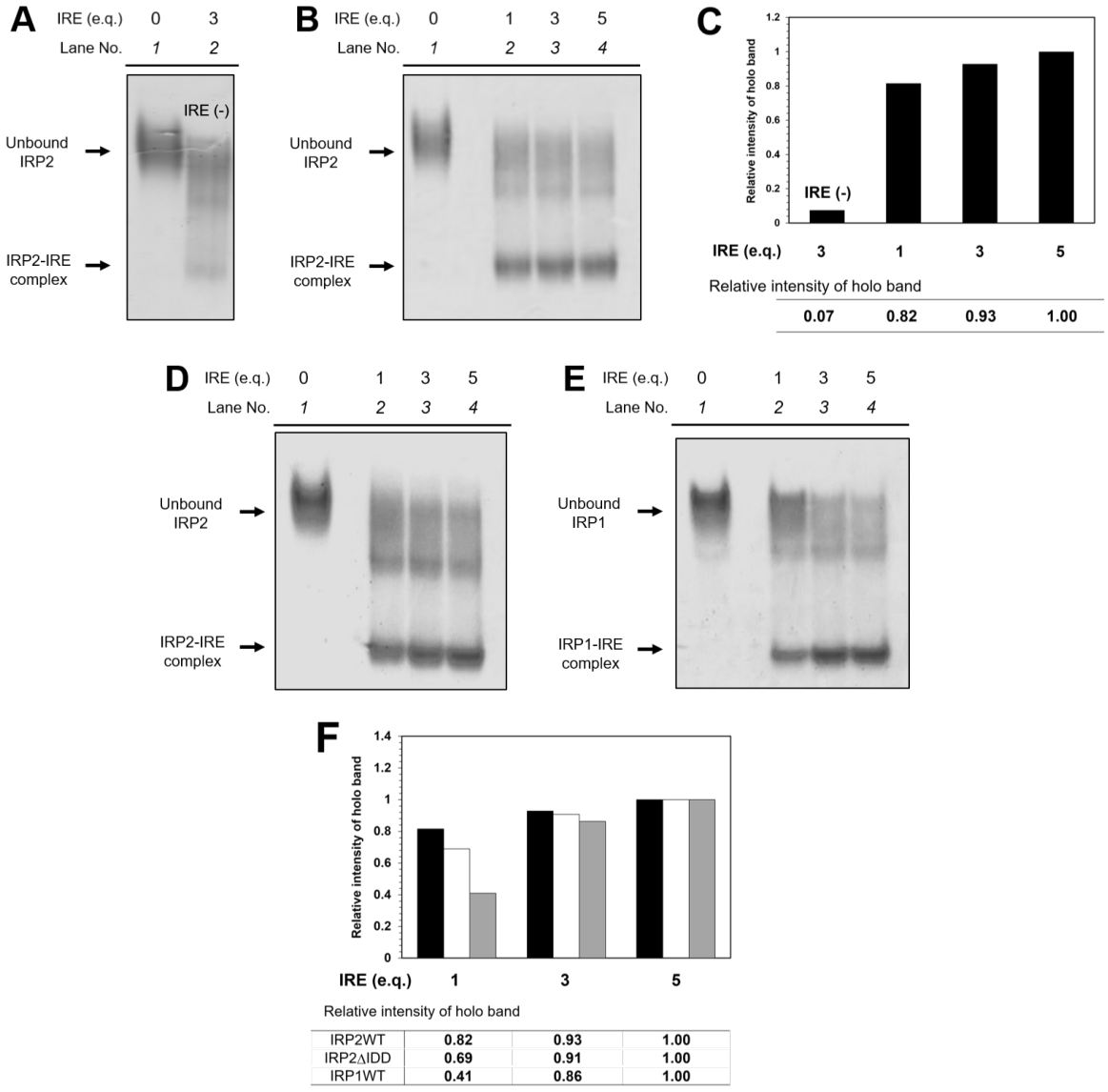

Figure 2.1 Native-PAGE for IRPs-IRE complex.

(A) CBB-stained gel image of Native-PAGE of free WT IRP2 (lane *1*) and WT IRP2 with three equivalent of IRE (-) (lane *2*). (B, D, E) WT IRP2 (B), IRP2ΔDD (D) and WT IRP1 (E) with/without IRE were loaded into each well in gel followed by running and staining by CBB. Gel images were obtained by scanning the gel immediately after washing with water. Free IRPs (lane *1*) and IRPs with one, three or five equivalents of IRE (lane *2*, *3*, *4*, respectively) were loaded in each gel. (C) Relative intensity of holo band for lane *2* of (A) and lane *2*,*3* and 4 of (B) quantified using Image J software. (F) Relative intensity of holo band for lanes *2*,*3* and 4 of (B), (D) and (E).

2.3.2. The Effect of Heme Binding on IRPs-IRE Complex Formation

To further examine the effects of heme binding on the binding affinity of IRPs to IRE by assessing the formation of the IRP-IRE complexes, we performed native PAGE analysis in the presence of heme. The addition of heme before mixing with IRE (heme-pretreated) (lanes *5–9*; Fig. 2.2A and F) increased the relative band intensity of IRE-unbound IRP1 with a compensation in the band intensity of the IRP1-IRE complex in the presence of heme. The increase in band intensity of IRE-unbound IRP1 in the presence of heme implied that the heme binding to IRP1 interferes with IRP1-IRE complex formation. However, the addition of heme to the IRP1-IRE complex induced mild perturbation of the relative band intensities of IRE-unbound and -bound IRP1, demonstrating that more than 50% of IRP1 was yet bound to IRE in the presence of heme (lanes *10* and *11*; Fig. 2.2A). Therefore, the heme binding affinity of IRP1 depends on the binding of IRE, and the heme binding affinity of the IRP1-IRE complex was relatively lower than that of IRE-unbound IRP1.

As described in the Chapter I, IRP1 has two heme binding sites; Cys118 and Cys300. To determine the heme binding site responsible for the heme-induced inhibition of the IRP1-IRE complex formation, native PAGE analyses for two Cys mutants, IRP1/C118A and IRP1/300A, were performed. By the addition of five heme equivalents to IRP1/C118A before the complex formation with IRE (heme-pretreated), the band intensity of the complex was decreased to 48% (lane *8*; Fig. 2.2B and F), which is higher than that of the WT IRP1 complex (30%) (lane *8*; Fig. 2.2A and F). IRE also partially dissociated from both WT IRP1 and IRP1/C118A by the addition of heme after the complex formation (IRE-pretreated) (lane *11*; Fig. 2.2A, B, and F). Furthermore, the mutation at Cys300 more substantially increased the band intensity of IRE-bound IRP1 in the presence of heme (30 % and 67 % for WT IRP1 and IRP1/C300A, respectively in the presence of five heme equivalents) (lane *8*; Fig. 2.2A, C and F), indicating that the heme binding to Cys300 in IRP1 is more effective in inhibiting the complex formation with IRE. The addition of heme after the complex formation did not induce the dissociation of

IRE at all (lane *11*; Fig. 2.2C and F). The dissociation of IRE from IRP1 is, therefore, predominantly induced by the heme binding at Cys300. Based on the crystal structure of IRE-bound IRP1 showing that Cys300 is positioned close to the IRE-binding site [23], the heme binding to Cys300 in IRP1 would sterically interfere the binding to IRE. Even in the presence of ten heme equivalents, however, the band intensity for the IRP1/C300A-IRE complex was reduced to 60% and the band for IRE-unbound IRP1/C300A was detected (lane *10*; Fig. 2.2C and F), indicating that the heme binding at Cys118 also affects the regulation of the IRP1-IRE complex formation.

Although the band of IRE-unbound IRP2 was unclear because of the structural instability of IRP2, the addition of heme to IRP2 more severely inhibited IRP2-IRE complex formation. In the presence of five heme equivalents, 30% and 3% of IRP1 and IRP2 formed a complex with IRE, respectively (lane *8*; Fig. 2.2D and F), revealing that the heme binding to IDD HRM more effectively inhibited IRP2-IRE complex formation. Another distinct difference was detected with regard to the addition of heme to the IRP2-IRE complex: the addition of heme drastically decreased the band intensity of the IRP2-IRE complex (14%) compared with that of the IRP1-IRE complex (57%, lane *11*; Fig. 2.2A, D and F). The heme binding to the IRP2-IRE complex enhanced the dissociation from IRE. Because the migration patterns for IRP2ΔIDD in the presence of heme were considerably similar to those of IRP1 before (30% and 22% for the IRP1- and IRP2ΔIDD-IRE complex in the presence of five heme equivalents, respectively) and after complex formation (57% and 50% for the IRP1- and IRP2ΔIDD-IRE complex in the presence of five heme equivalents, respectively) (Fig. 2.2A, E and F), the difference in the migration pattern of IRP2 and IRP1 originated from the heme binding to IDD HRM of IRP2. We also tried to determine the essential heme binding site for the inhibition of the complex formation between IRP2 and IRE, but the Cys mutants in IRP2 showed smear bands for the

native PAGE analysis owing to instability of the protein, and thus we could not determine the effect of mutation at Cys of IRP2 in heme-mediated regulation.

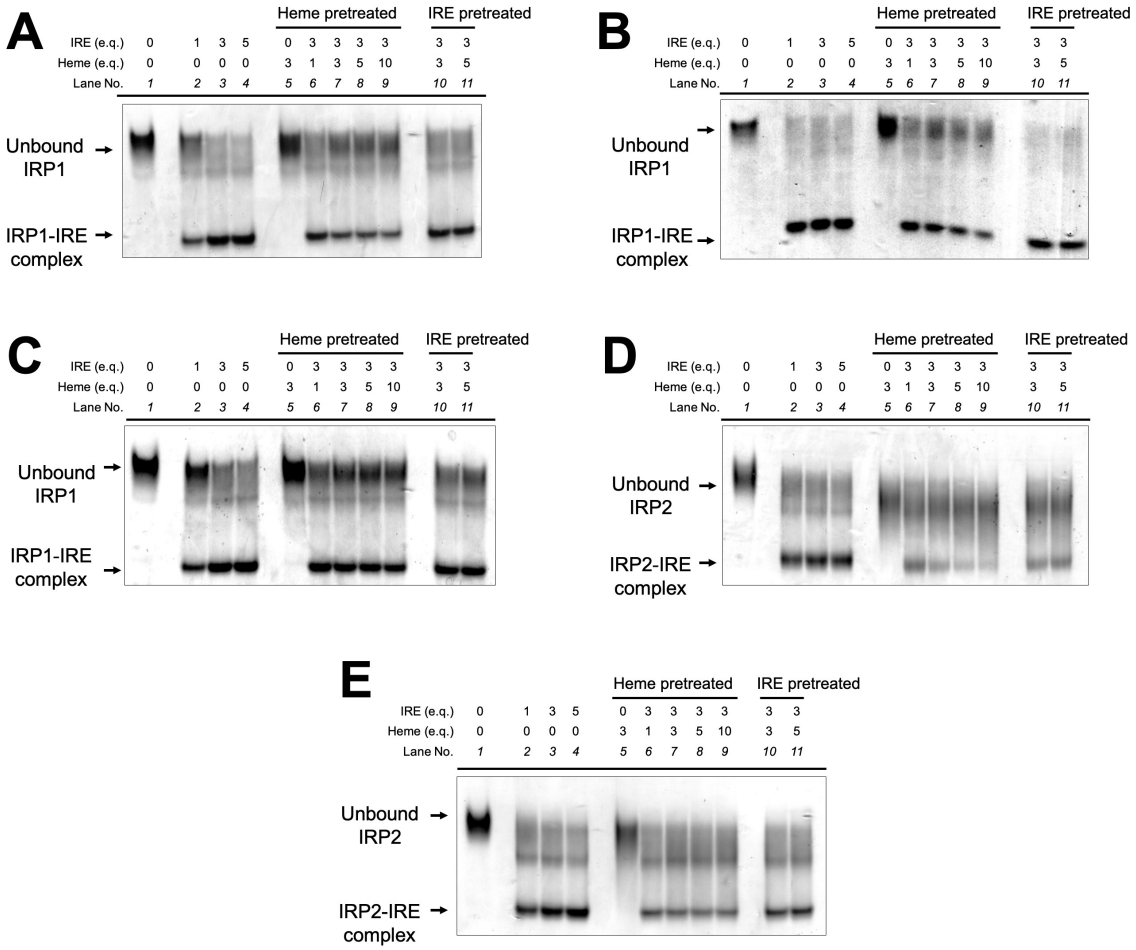

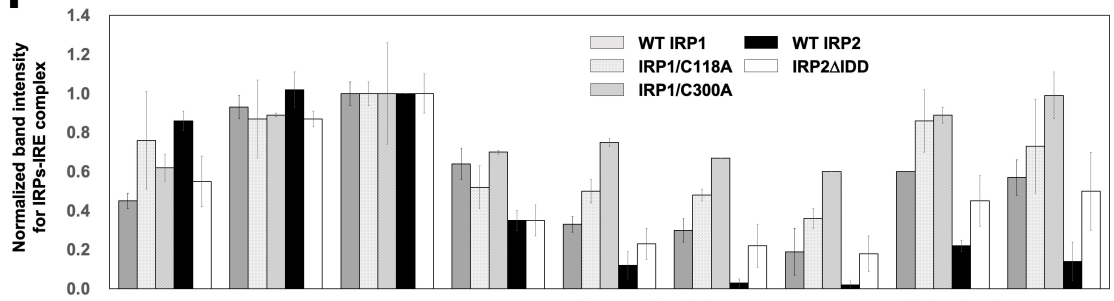

Normalized band intensity for IRPs-IRE complex

				Heme pretreated				IRE pretreated	
IRE (e.q.)	1	3	5	3	3	3	3	3	3
Heme (e.q.)	0	0	0	1	3	5	10	3	5
WT IRP1	0.45±0.04	0.93±0.06	1.00±0.06	0.64±0.08	0.33±0.04	0.30±0.06	0.19±0.12	0.60±0.00	0.57±0.09
IRP1/C118A	0.76±0.25	0.87±0.20	1.00±0.06	0.52±0.11	0.50±0.06	0.48±0.03	0.36±0.05	0.86±0.16	0.73±0.24
IRP1/C300A	0.62±0.07	0.89±0.01	1.00±0.26	0.70±0.01	0.75±0.02	0.67±0.00	0.60±0.00	0.89±0.04	0.99±0.12
WT IRP2	0.86±0.05	1.00±0.09	1.00±0.00	0.35±0.05	0.12±0.07	0.032±0.024	0.018±0.018	0.22±0.03	0.14±0.10
IRP2ΔIDD	0.55±0.13	0.87±0.04	1.00±0.10	0.35±0.08	0.23±0.08	0.22±0.11	0.18±0.09	0.45±0.13	0.50±0.20

Figure 2.2 Native-PAGE for IRPs-IRE complex in the presence of heme

Coomassie brilliant blue (CBB)-stained gel images of native PAGE for WT IRP1 (A), IRP1/C118A (B), IRP1/C300A (C), WT IRP2 (D), and IRP2ΔIDD (E). IRPs [lane *1*], IRPs and IRE complex [lanes *2–4*], heme-pretreated IRPs and IRE [lanes *5–9*], and IRE-pretreated IRPs and heme [lanes *10* and *11*] were loaded into each well of the gel followed by electrophoresis and CBB staining. Gel images were obtained by scanning the gel immediately after washing with water. (F) Band intensities of the total proteins and IRP-IRE complexes (holo band intensity) in each lane were quantified using the Image J software (http://rsb.info.nih.gov/ij). Relative intensity of the holo band is calculated from the ratio of holo band intensity to total band intensity in each well and then normalized to the relative intensity of holo band in lane *4* containing IRPs and five IRE equivalents. The data points and error bars represent the means and standard errors of two independent experiments using two different protein preparations.

2.3.3. The Effect of Heme Binding to IRPs on Their Secondary Structures.

The gel shift assay experiments clearly showed that the heme binding to IRPs inhibited the IRE binding. The heme induced inhibition of the substrate binding was also encountered for a heme-regulated transporter regulator, HrtR (*16*). In this protein, the heme binding induces the relative positions of α-helices, resulting in the significant changes in the circular dichroism (CD) spectrum. In addition, the significant alterations of CD spectra of IRP1 upon assembly with [4Fe-4S] cluster, and both of IRP1 and IRP2 by addition of IRE were previously reported (*17, 18*). These facts suggest the possibility of heme-induced conformational changes in IRPs by changing the secondary structure.

To examine the conformational changes associated with the heme binding to IPRs, we followed the spectral changes in the CD spectra by the addition of heme to IRPs. As shown in Fig. 2.3A-C, all of the CD spectra exhibited a troughs at 208 and 222 nm, indicative of the α-helix structures, as previously observed (*17, 18*). The ellipticity around 208 and 222 nm for IRPs were slightly decreased upon heme binding. However, the changes in ellipticity for IRPs in the presence of heme were much smaller than that previously found in IRP1 with [4Fe-4S] cluster and IRPs with IRE association, or in HrtR by heme binding (*16-18*), suggesting the only small changes of secondary structure in IRPs upon the binding of heme to HRMs. Although we cannot exclude the possibility of the heme-induced conformational changes in IRPs, significant changes in the relative positions of α-helices observed for HrtR was not induced by the heme binding to IRPs.

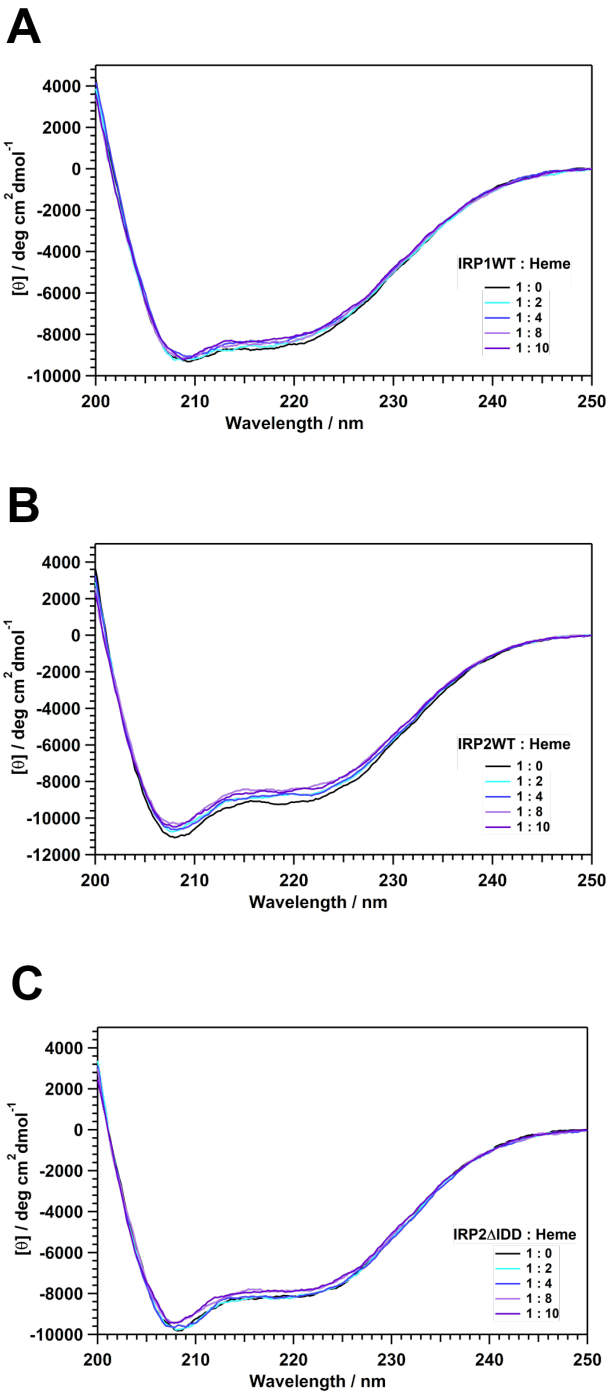

Figure 2.3 CD spectra of IRPs in the absence and presence of heme

CD spectra of WT IRP1 (A), WT IRP2 (B) and IRP2ΔIDD (C) with or without heme. CD spectra in the far-UV region for 2 μM IRPs in 50 mM Tris-HCl (pH 7.4). Molar and mean residue ellipticity was calculated based on the molar concentration of samples and the number of amino acids.

2.4. Discussion

2.4.1 Heme-mediated Inhibition of IRPs-IRE Complex Formation

As we previously reviewed (*19*), the function of many proteins containing HRM are altered or regulated by reversible heme binding to HRM. In addition to the heme-mediated regulation of IRP2 that has already been discussed, previous study also found that both IRP1 and IRP2 specifically bind to heme via their HRMs consisting of Cys-Pro dipeptides (*10*), indicating the heme-mediated regulation of both IRPs through heme binding to their conserved HRMs. In this paper, I investigated the impact of heme binding to HRMs in IRPs on the complex formation with IRE and their structure. Firstly, I successfully detected the complex formation of IRPs-IRE using native PAGE (Fig. 2.1). In these results, the rate of IRPs-IRE complex formation for WT IRP1 (0.41) was slightly lower than that for WT IRP2 (0.82) and IRP2ΔIDD (0.69) in the presence of one equivalent of IRE. As only IRP1 forms the homo-dimer, which is not suitable for complex formation with IRE, in the low micromolar range (*18*), under the experimental conditions in this paper the rate of complex formation of IRP2 with IRE would be higher than that of IRP1 with one equivalent of IRE, which is not sufficient for saturation of IRPs as complex. On the other hand, no significant differences for the rate of complex formation with IRE were observed between WT IRP2 and IRP2ΔIDD, implying that the IDD domain would not be involved in the association with IRE. This suggestion corresponds to the result from the previous study reporting that the deletion of IDD domain in IRP2 did not measurably alter the affinity with IRE, confirmed by EMSA assay (*20*).

I in turn assess the effect of heme binding to HRMs in IRPs on complex formation with IRE (Fig. 2.2). The rate of complex formation was decreased by the addition of heme to IRP1 before the complex formation with IRE, demonstrating that the heme inhibits the association of IRP1 with IRE (Fig. 2.2A). Here, we considered the role of HRMs in IRP1 based on the crystal structure of IRP1 with ferritin IRE (Fig. 2.4). In the structure of IRP1, the HRM consisting of

Cys300-Pro301 is placed next to the Glu302, which makes the stacking interaction with U17 in ferritin IRE (*14*). The previous study focusing on the alteration on interactions between IRP1 and IRE by mutagenesis in IRP1 revealed that the stacking of Glu302 in IRP1 with IRE stabilizes the IRP1-IRE complex and interference of this bond largely decreased the affinity for the interactions (*21*). These facts indicates that the heme binding to Cys300 in IRP1 or corresponding Cys in IRP2 (Cys120) induces the steric inhibition by disrupting the interaction between Glu302 of IRP1 and U17 in IRE.

In contrast to the native PAGE for IRP1 with IRE in the presence of heme, the heme binding to HRM in IDD domain of IRP2 have larger effect on the inhibition of IRPs-IRE complex formation than the HRMs in IRP1 or HRMs outside the IDD domain in IRP2 (Fig. 2.2B). Moreover, despite the no significant effect of the addition of heme to pre-formed IRP1-IRE complex, heme seems to be able to bind to HRM of the IDD domain in IRP2-IRE complex, resulting in the association of IRP2 from IRE. Given that the IDD domain in IRP2 does not contribute to the association with IRE as described above and reported in previous study (*20*), the heme binding to HRM in IDD domain may not cause the steric inhibition of IRP2-IRE complex formation and rather promotes the dissociation of IRP2 as a non-competitive inhibitor (*22*). Since the HRM in IDD domain is the allosteric site compared to the IRE binding sites, the heme binding to the HRM in IDD domain possibly induces the conformational changes in IRP2, as found by the binding of the various non-competitive inhibitor (*23, 24*).

The CD spectra of WT IRP1, WT IRP2 and IRP2ΔIDD, however, exhibited no significant changes in their secondary structure upon addition of heme. Thus, although I cannot exclude the possibility of heme-induced structural changes in IRPs, no significant conformational changes in IRPs occurred. If some conformational changes happen in IRPs upon heme binding, it would be only small perturbation in the entire protein structure or local structural change without affecting the secondary structures. To suspect the mechanism for the heme-induced

conformation changes in IRPs, particularly in IRP2 whose complex formation with IRE seems to be allosterically inhibited by heme binding, we considered the heme binding environment including the ligands of heme. Our previous study revealed that heme binding site of IRPs consist of both five-coordinate with by cysteine and six-coordinate with by cysteine and histidine (*10*). While Cys201 in the IDD domain is one of the ligands for ferric heme, another histidine ligand for ferric heme in IRP2 have not been identified (*1*). Since there is only one histidine (His204) in the IDD domain, to which axial ligand for heme is replaced from Cys201 by the reduction of heme-iron (*1*), the axial ligand for six-coordinate ferric heme would be Cys201 in IDD domain and unidentified histidine outside IDD domain. As the six-coordination geometry requires two distinct amino acid ligands coordinating to heme, formation of six-coordinate heme could induce conformational changes in the protein, as found in a heme-dependent transcription factor Bach2 (*25*), mouse heme-regulated eukaryotic initiation factor 2α kinase (HRI) (*26*) and porphobilinogen deaminase from *Vibrio cholerae* (*27*). Given the two ligands placed in different domains for ferric heme, the formation of the six-coordinate heme at HRM in IDD domain might also induce structural changes in IRP2. This suggestion for conformational changes would be supported by the intrinsically flexible structure of IDD domain which was predicted by using DISOPRED2 based on its amino acid sequences (Fig. 2.5).

Thus, we concluded that heme binding to HRMs outside IDD domain sterically inhibits the IRPs-IRE complex formation, whereas heme bound to HRM in IDD domain causes dissociation from IRE probably owing to the formation of six-coordinate heme and the flexibility of IDD domain, resulting in the conformational changes in IRP2.

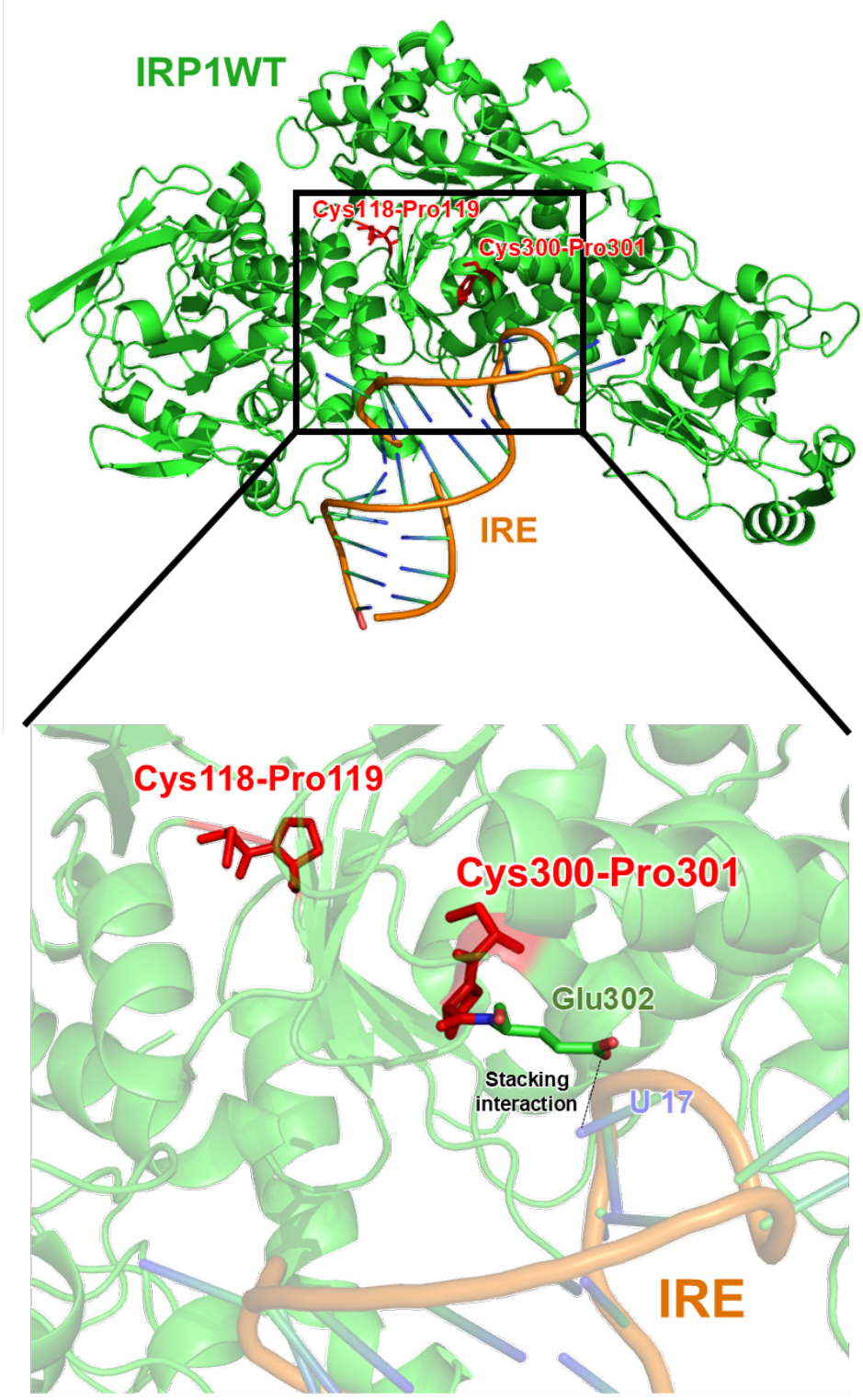

Figure 2.4 Crystal structure of IRP1 with ferritin IRE (PDB ID: 3SNP).
CP motifs and Glu302 showing the stacking interaction (depicted as dotted line) with U17 in IRE are highlighted in red and green, respectively.

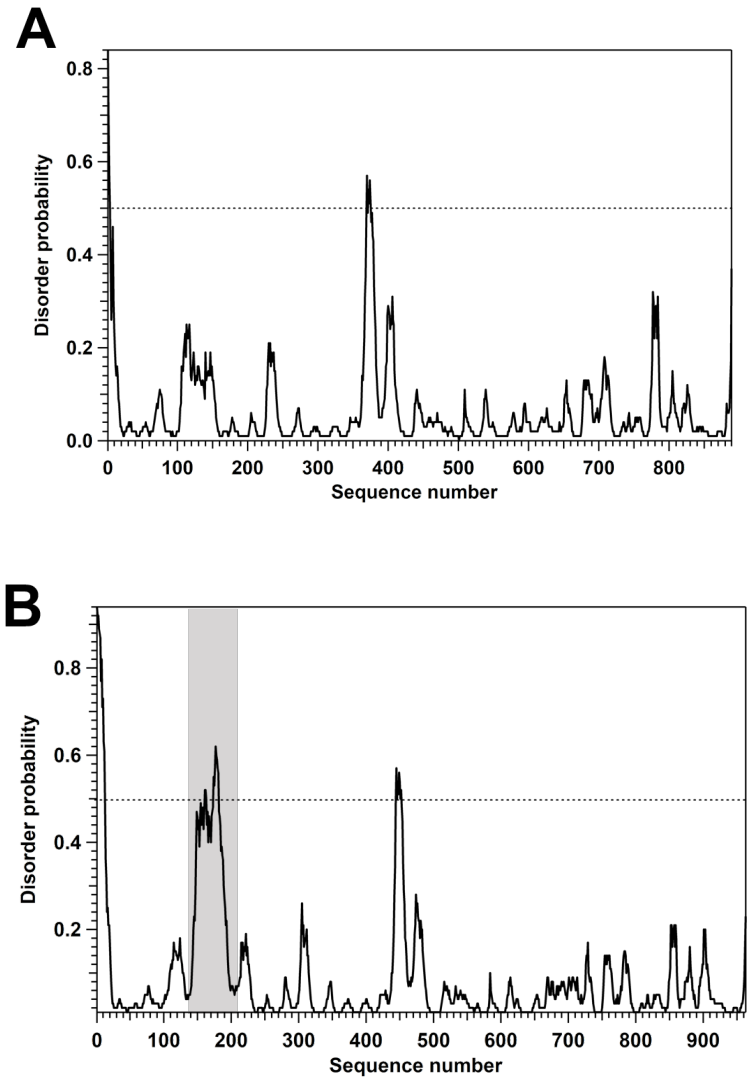

Figure 2.5. Disorder profiles of IRP1 and IRP2 amino acid sequence.

The plot shows the sequence number of IRP1 (A) and IRP2 (B) against probability of disorder obtained using DISOPRED2. The amino acid sequence of the IDD domain (137–209) in IRP2 is highlighted by gray.

2.4.2 Physiological Importance of Heme-mediated Inhibition of IRPs-IRE complex formation

In this chapter, I clearly revealed that ferric (Fe^{3+}) heme inhibits the complex formation of IRPs-IRE *in vitro*. In mammalian cells, IRPs are cytosolic proteins (*28, 29*), so that they would bind cytosolic heme via their HRMs. Although the cellular heme is supposed to exist as both of inert heme that is more abundant and associated with high-affinity hemoproteins like cytochrome *c* and globins, and labile heme pool that can reversibly bind to proteins, the property of intracellular labile heme is poorly understood (*30, 31*). While heme might be biased toward its reducing form because of the reducing environment in cytosols (*32*), reduced heme is more cytotoxic (*33, 34*), suggesting that the intracellular heme is buffered by unknown factor (*35*). Taken together, sensing of ferric heme, not ferrous (Fe^{2+}) heme, at Cys residue of HRMs may be important to avoid the cytotoxicity of heme, implying that IRPs bind to the ferric labile heme, which is possibly transported by other molecules, leading to the inhibition of complex formation with IRE.

References

1. H. Ishikawa *et al.*, Involvement of heme regulatory motif in heme-mediated ubiquitination and degradation of IRP2. *Mol Cell* **19**, 171-181 (2005).
2. J. Dupuy *et al.*, Crystal structure of human iron regulatory protein 1 as cytosolic aconitase. *Structure* **14**, 129-139 (2006).
3. K. Yamanaka *et al.*, Identification of the ubiquitin-protein ligase that recognizes oxidized IRP2. *Nat Cell Biol* **5**, 336-340 (2003).
4. X. D. Tang *et al.*, Haem can bind to and inhibit mammalian calcium-dependent Slo1 BK channels. *Nature* **425**, 531-535 (2003).
5. S. Raghuram *et al.*, Identification of heme as the ligand for the orphan nuclear receptors REV-ERB alpha and REV-ERB beta. *Nat Struct Mol Biol* **14**, 1207-1213 (2007).
6. J. Igarashi *et al.*, Elucidation of the heme binding site of heme-regulated eukaryotic initiation factor 2 alpha kinase and the role of the regulatory motif in heme sensing by spectroscopic and catalytic studies of mutant proteins. *Journal of Biological Chemistry* **283**, 18782-18791 (2008).
7. J. Shen *et al.*, Iron Metabolism Regulates p53 Signaling through Direct Heme-p53 Interaction and Modulation of p53 Localization, Stability, and Function. *Cell Reports* **7**, 180-193 (2014).
8. C. Kitatsuji *et al.*, Protein oxidation mediated by heme-induced active site conversion specific for heme-regulated transcription factor, iron response regulator. *Sci Rep* **6**, 18703 (2016).
9. K. Iwai *et al.*, Iron-dependent oxidation, ubiquitination, and degradation of iron regulatory protein 2: implications for degradation of oxidized proteins. *Proc Natl Acad Sci U S A* **95**, 4924-4928 (1998).
10. M. Ogura *et al.*, Redox-dependent axial ligand replacement and its functional significance in heme-bound iron regulatory proteins. *J Inorg Biochem* **182**, 238-248 (2018).
11. H. OKUTANI, Heme binding controls the function of Iron Regulatory Protein (IRP). *Master Thesis*, (2011).
12. R. M. C. Dawson, D. C. Elliot, W. H. Elliot, K. M. Jones, Porphyrins and Related Compounds. *Data for Biochemical Research, Oxford University Press, Oxford*, pp. 314-317 (1974).
13. Y. W. Park, M. G. Katze, Translational control by influenza virus. Identification of cis-acting sequences and trans-acting factors which may regulate selective viral mRNA translation. *J Biol Chem* **270**, 28433-28439 (1995).
14. W. E. Walden *et al.*, Structure of dual function iron regulatory protein 1 complexed with ferritin IRE-RNA. *Science* **314**, 1903-1908 (2006).

15. B. R. Henderson, E. Menotti, C. Bonnard, L. C. Kuhn, Optimal sequence and structure of iron-responsive elements. Selection of RNA stem-loops with high affinity for iron regulatory factor. *J Biol Chem* **269**, 17481-17489 (1994).
16. H. Sawai, M. Yamanaka, H. Sugimoto, Y. Shiro, S. Aono, Structural basis for the transcriptional regulation of heme homeostasis in Lactococcus lactis. *J Biol Chem* **287**, 30755-30768 (2012).
17. X. Brazzolotto, P. Timmins, Y. Dupont, J. M. Moulis, Structural changes associated with switching activities of human iron regulatory protein 1. *J Biol Chem* **277**, 11995-12000 (2002).
18. E. Yikilmaz, T. A. Rouault, P. Schuck, Self-association and ligand-induced conformational changes of iron regulatory proteins 1 and 2. *Biochemistry* **44**, 8470-8478 (2005).
19. K. Ishimori, Y. Watanabe, Unique heme environmental structures in heme-regulated proteins using heme as the signaling molecule. *Chem Lett* **43**, 1680-1689 (2014).
20. J. Butt *et al.*, Differences in the RNA binding sites of iron regulatory proteins and potential target diversity. *Proc Natl Acad Sci U S A* **93**, 4345-4349 (1996).
21. A. I. Selezneva, W. E. Walden, K. W. Volz, Nucleotide-specific recognition of iron-responsive elements by iron regulatory protein 1. *J Mol Biol* **425**, 3301-3310 (2013).
22. R. R. Ramsay, K. F. Tipton, Assessment of Enzyme Inhibition: A Review with Examples from the Development of Monoamine Oxidase and Cholinesterase Inhibitory Drugs. *Molecules* **22**, (2017).
23. J. A. Macpherson, D. Anastasiou, Allosteric regulation of metabolism in cancer: endogenous mechanisms and considerations for drug design. *Curr Opin Biotechnol* **48**, 102-110 (2017).
24. C. J. Wenthur, P. R. Gentry, T. P. Mathews, C. W. Lindsley, Drugs for allosteric sites on receptors. *Annu Rev Pharmacol Toxicol* **54**, 165-184 (2014).
25. M. Watanabe-Matsui *et al.*, Heme binds to an intrinsically disordered region of Bach2 and alters its conformation. *Arch Biochem Biophys* **565**, 25-31 (2015).
26. J. Igarashi *et al.*, Elucidation of the heme binding site of heme-regulated eukaryotic initiation factor 2alpha kinase and the role of the regulatory motif in heme sensing by spectroscopic and catalytic studies of mutant proteins. *J Biol Chem* **283**, 18782-18791 (2008).
27. T. Uchida, T. Funamizu, M. Chen, Y. Tanaka, K. Ishimori, Heme Binding to Porphobilinogen Deaminase from Vibrio cholerae Decelerates the Formation of 1-Hydroxymethylbilane. *ACS Chem Biol* **13**, 750-760 (2018).
28. S. M. Patton, D. J. Pinero, N. Surguladze, J. Beard, J. R. Connor, Subcellular localization of iron regulatory proteins to Golgi and ER membranes. *J Cell Sci* **118**, 4365-4373 (2005).

29. D. J. Pinero, N. Li, J. Hu, J. L. Beard, J. R. Connor, The intracellular location of iron regulatory proteins is altered as a function of iron status in cell cultures and rat brain. *J Nutr* **131**, 2831-2836 (2001).
30. S. Severance, I. Hamza, Trafficking of Heme and Porphyrins in Metazoa. *Chemical Reviews* **109**, 4596-4616 (2009).
31. D. A. Hanna *et al.*, Heme dynamics and trafficking factors revealed by genetically encoded fluorescent heme sensors. *Proc Natl Acad Sci U S A* **113**, 7539-7544 (2016).
32. J. J. Hu, L. X. Dong, C. E. Outten, The Redox Environment in the Mitochondrial Intermembrane Space Is Maintained Separately from the Cytosol and Matrix. *Journal of Biological Chemistry* **283**, 29126-29134 (2008).
33. V. Jeney *et al.*, Pro-oxidant and cytotoxic effects of circulating heme. *Blood* **100**, 879-887 (2002).
34. F. A. D. T. G. Wagener *et al.*, Heme is a potent inducer of inflammation in mice and is counteracted by heme oxygenase. *Blood* **98**, 1802-1811 (2001).
35. S. Sassa, Why heme needs to be degraded to iron, biliverdin IX alpha, and carbon monoxide? *Antioxid Redox Sign* **6**, 819-824 (2004).

CHAPTER III

DETECTION OF HEME-MEDIATED OXIDATION OF IRP2 AND IDENTIFICATION OF THE ROS

ABSTRACT

In chapter II, I clearly found that heme binding to HRMs in both IRPs inhibits the complex formation with IRE. While the heme bound to the HRM near the IRE binding site would sterically inhibit the interaction of IRPs with IRE, the heme binding to HRM in the IDD domain causes the larger effect on the inhibition to the complex between IRP2 and IRE, and also induces the dissociation of IRP2 from IRE. Therefore, although I revealed that the heme can functionally regulate both IRPs by binding to HRMs, the roles of each HRM in IRPs in heme-mediated regulation are different. The heme-mediated degradation of IRP2 induced by heme binding to HRM in the IDD domain has also been reported as a specific reaction of IRP2. Although the heme binding to the IDD domain would trigger the induction of oxidative modification in IRP2, the molecular mechanism for the oxidation of IRP2 has not been understood.

In chapter III, I focused on the investigation of the heme-mediated oxidation in IRP2. I proved that the *in vitro* heme-mediated oxidation was observed in WT IRP2, but not in WT IRP1 or IRP2ΔIDD, demonstrating that the IDD domain is required for heme-mediated oxidation in IRP2. As the addition of catalase suppressed the oxidation, H_2O_2 is supposed to be generated and involved in the oxidation of IRP2. Although the heme degradation by H_2O_2 and subsequent non-heme iron release are important for heme-mediated oxidation in Irr, the non-heme iron does not seem to be responsible for oxidation in IRP2, suggesting that H_2O_2 would be activated by reacting with heme-iron, instead of non-heme iron, which is produced following the heme degradation. Given that the H_2O_2 production was also observed in WT IRP1 or IRP2ΔIDD, the H_2O_2 generated on the heme at HRM in IDD domain would readily consumed to be activated into more reactive species, such as ·OH.

3.1. Introduction.

I clearly revealed the functional role of heme in IRPs-IRE complex formation, as described in chapter II. While the interactions of IRE with IRP1 and IRP2 are inhibited by binding of heme to their HRMs, the heme bound to HRM in IDD domain exhibited more significant effect on the inhibition of the complex formation with IRE and even induces the dissociation of IRP2 from IRE. Thus, the different roles of each HRMs in IRP1 and IRP2 have been proposed, which differentiates the heme-mediated regulation of their function.

In addition to the heme-induced inhibition of IRPs-IRE complex formation described above, the heme-mediated degradation through the IDD domain have also been reported and examined (*1-6*). In an iron-replete condition, IRP2 is sensitive to its degradation, whereas the removal of the IDD domain stabilizes IRP2 in iron sufficient cells (*1, 3*). In this condition, the oxidative modification in IRP2 was detected and the oxidation of IRP2 seems to be required for the recognition by ubiquitin ligase, HOIL-1, which leads to proteasomal degradation of IRP2 (*3, 4*). As previously reported, addition of heme to the cell lysate containing IRP2 resulted in the oxidative modification of the protein, which leads to the protein degradation in the proteasome, but such oxidative modification was not detected in an IRP2 mutant lacking the IDD domain, IRPΔIDD, and IRP1 (*6*). Although these facts supposed that the oxidative modification in IRP2 is s triggered by the heme binding to HRM in the IDD domain, the molecular mechanism remains unclear.

In this chapter III, I successfully found that WT IRP2 is subject to the *in vitro* heme-mediated oxidation in the presence of reductant, DTT, but WT IRP1 and IRP2ΔIDD are not. Therefore the IDD domain is responsible for the heme-mediated oxidation in IRP2. This oxidative modification was moderately suppressed by the addition of catalase, the quencher of H_2O_2, indicating the production and involvement of H_2O_2 in the oxidation of IRP2. Although the production of H_2O_2 from heme-loaded WT IRP2 was confirmed, heme in WT IRP1 and

IRP2ΔIDD also generates the similar amount of H_2O_2 to WT IRP2, implying the produced H_2O_2 at the HRM in the IDD domain would be immediately activated into more reactive species. The Oxyblot analysis also revealed that the oxidation of IRP2 is not caused by non-heme iron, as observed in Irr (*8*). Therefore, it is suggested that the H_2O_2 generated in the heme at HRM in the IDD domain is activated by heme-iron, leading to the generation of more reactive species, ·OH.

3.2. Experimental Procedures.

3.2.1 Materials.

All chemicals were purchased from Wako Pure Chemical Industries (Osaka, Japan), Nacalai Tesque (Kyoto, Japan) or Sigma-Aldrich (St. Louis, MO, USA), and used without further purification.

3.2.2 Protein Expression and Purification

The procedure for the expression and purification of IRPs are described in Chapter II.

3.2.3 *In Vitro* Protein Oxidation Analysis.

Purified IRPs were diluted to 5 μM in 50 mM HEPES buffer and incubated with the three and two equivalent amounts of hemin for WT IRP2, and WT IRP1/IRP2ΔIDD, respectively. The IRPs solution were mixed with or without ROS scavengers; 20 mM mannitol or 1,000 units/ml catalase from bovine liver (Wako) dissolved in 50 mM HEPES buffer. The *in vitro* oxidation reactions for IRPs were initiated by addition of 2 mM DTT (dithiothreitol) on ice.

The Oxyblot protein oxidation detection kit (Merck) was used to detect oxidized carbonyl groups derived from oxidation of amino acid residue (*7*). The procedure for the Oxyblot analysis, including the derivatization of protein, electrophoresis, immunoblot analysis was performed as described in our previous paper (*8*), except the 7.5 % (w/v) e-PAGEL polyacrylamide gels (Atto) used for IRPs.

The enhancement of chemiluminescence by the incubation of blotted membranes with the working solution containing luminol and peroxide (Nacalai tasque) was followed by visualization with a ImageQuant LAS 4000 mini CCD camera (Fujifilm). The immunoblot

images of the membranes were obtained with increment exposure at 1 min intervals up to 30 min. All images on this chapter were obtained at 30 min exposure. The band intensities of oxidized IRPs after the DTT treatment were subtracted from the intensities of the samples at 0 min. The subtracted intensities were expressed relative to the maximum band intensity of the reaction of IRP2 in the presence of heme and reductant (60 or 90 min after the initiation of the reaction), which was normalized to a value of 1.0.

3.2.4 Spectroscopic Assay for the Detection of H_2O_2 Production in the Presence of Heme and Reductant.

To quantify the production of hydrogen peroxide from heme-bound IRPs, we used a Quantitative Peroxide Assay Kit (Pierce) as previously reported (*9*). The purified IRPs (5 μM) in 50 mM HEPES buffer were incubated with an excess amount of heme (5 equivalents) in DMF for 10 min, followed by the cleaning up through a Bio-Spin column with Bio-Gel P-30 (BioRad) to remove free hemin. 50 μl of this mixture was mixed with 2 mM DTT and left on ice for 20 min. After the incubation, the detection of H_2O_2 were carried out as previously reported (*8*). We quantified the amount of H_2O_2 by the absorbance at 595 nm with an extinction coefficient (ε_{595}) of 1.5×10^4 $M^{-1}cm^{-1}$.

3.2.5 Spectroscopic Measurement for Heme-loaded IRPs with PDTS

The three equivalents of hemin in DMF was added into purified 5 μM IRPs and the excess free heme was removed using Bio-Spin column (Bio-Gel P-30, BioRad). The 100 μL mixture was loaded onto the column, which was pre-washed three times with 50 mM HEPES buffer. The eluent of the column was collected by centrifugation at 1,000 g for 1 minute. The collected solution containing heme-loaded IRP2 was diluted 5 fold with 50 mM HEPES/100 mM NaCl

(pH 7.4). The solution was mixed with the 100 μM of 3-(2-Pyridyl)-5,6-diphenyl-1,2,4-triazine-*p,p*'-disulfonic acid monosodium salt hydrate (PDTS), also known as ferrozine, which is colorimetric reagent used for ferrous (Fe^{2+}) iron quantification (*10*). PDTS specifically forms a complex with ferrous iron ions (Fe $[Ferrozine]_3^{4-}$), which contributes increased absorption at 562 nm. DTT at a final concentration of 2 mM was subsequently added to the solution to initiate the oxidation reaction. The absorbance at from 300 to 800 nm of this solution was measured at 5 minutes intervals up to 150 minute after addition of DTT using UV-VIS spectrophotometer V-660 (JASCO).

3.3. Results

3.3.1. Heme-induced Oxidative Modification in IRPs

To confirm the oxidative modification of purified IRPs, I examined the oxidation reaction of IRPs using Oxyblot in the presence of a reductant, DTT, under aerobic conditions (oxidative modification (OM) conditions) (Fig. 3.1A-C). As displayed in the Fig. 3.1A, bands derived from oxidized IRP2 appeared at ~100 kDa and the intensity of the bands increased over time after addition of DTT in the presence of heme. In contrast, IRP1 and IRP2ΔIDD did not show any clear bands at around 100 kDa (Fig. 3.1B, C), supporting our previous observation in cells that the heme binding to the IDD domain is required for the heme-mediated oxidation of IRP2.

Such heme-induced oxidative modification has been reported for Irr, a bacterial heme-regulated transcription factor (*8, 11, 12*). In the oxidative modification of Irr, previous report identified the formation of hydrogen peroxide (H_2O_2) and further activation of H_2O_2 to more reactive oxygen species (ROS) such as hydroxyl radical (·OH), which oxidizes the specific amino acid residues (*8*). As observed in Irr (*8*), the reactivity of H_2O_2 is not enough to directly oxidize amino acid residues in IRP2 (Fig. 3.1A), supporting further activation of H_2O_2 in IRP2. To determine the ROS involved in the oxidation of IRP2 and to clarify the mechanism of its production, I performed Oxyblot analysis under the OM conditions in the presence of ·OH scavenger (mannitol) (*13, 14*) and H_2O_2 scavenger (catalase). As shown in Fig. 3.2A, the addition of mannitol did not suppress the oxidative modification in IRP2, suggesting that ·OH is not produced, or is immediately consumed after the production. On the other hand, the addition of catalase moderately suppressed the oxidation of IRP2 until 30 min after the initiation of the oxidation reaction (Fig. 3.2B). The oxidation of IRP2 in the presence of catalase progressively increased more than 60 min after the reaction, probably due to the inactivation of catalase by ·OH (*15*). Moreover, ·OH generated from catalase in the presence of H_2O_2 may also contribute the progress of oxidation in IRP2 over long time after the

reaction initiated (*16*). Therefore, the production of H_2O_2 in the OM condition for IRP2 was proposed. Since the catalase also suppressed the heme-mediated oxidation of Irr (*8*), the oxidation of IRP2 might proceed via similar process to that for Irr (*8*). In the oxidation of Irr, the generated H_2O_2 promotes the degradation of heme resulting in the release of free iron, followed by the metal-catalyzed oxidation of amino acid around the non-heme iron binding site based on Fenton's reaction (*8, 17-20*). Thus, we further examined the confirmation of H_2O_2 production and metal-catalyzed oxidation of IRP2 under OM condition.

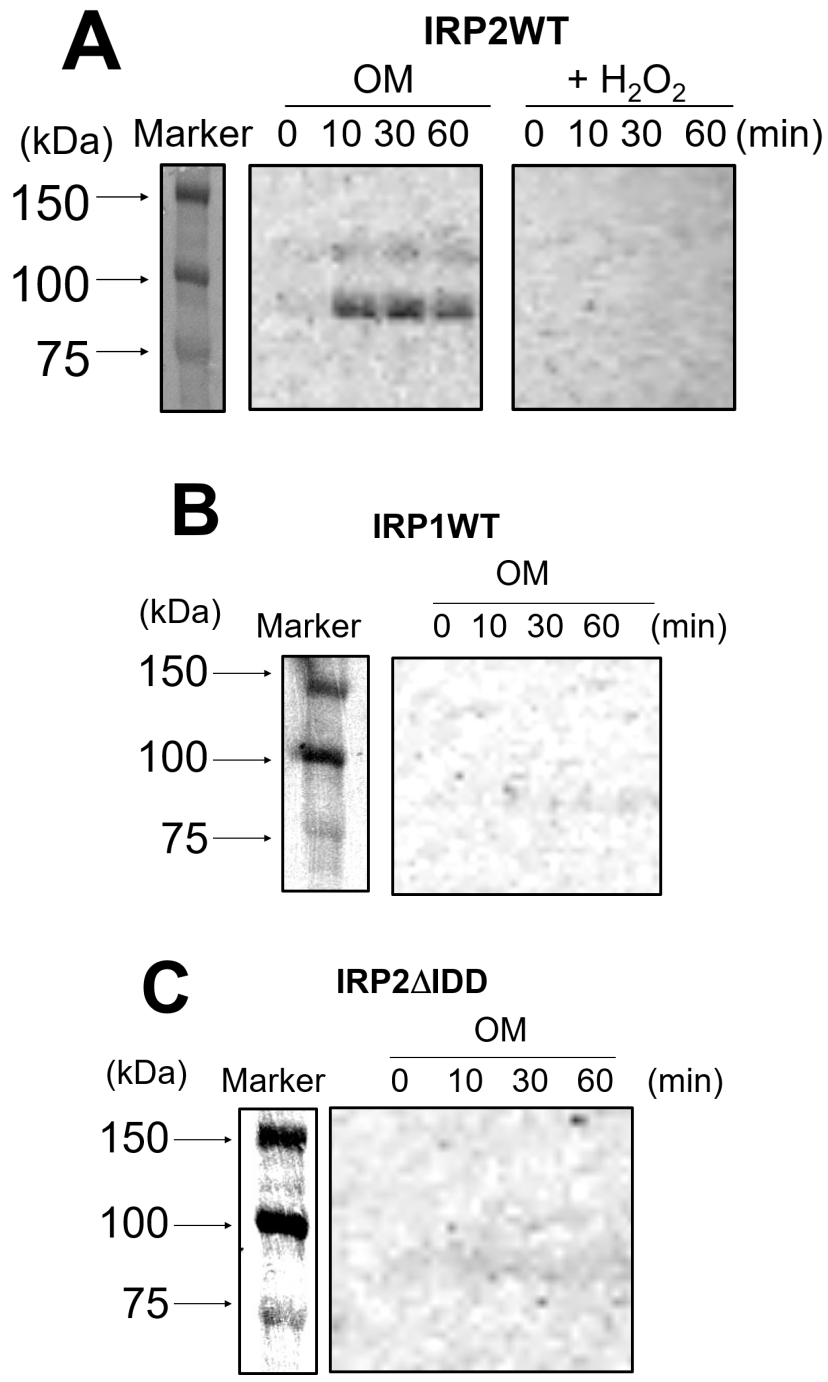

Figure 3.1 Oxyblot analysis of IRPs in the presence of heme and DTT.

The time course Oxyblot assay for the oxidation of WT IRP2WT IRP2 (A), WT IRP1 (B) and IRP2ΔIDD (C). 5 μM of IRPs were mixed with three equivalents of heme and oxidation was initiated by addition of 2 mM of DTT. (A) +H_2O_2: Addition of 2 mM H_2O_2 instead of the addition of heme and reductant

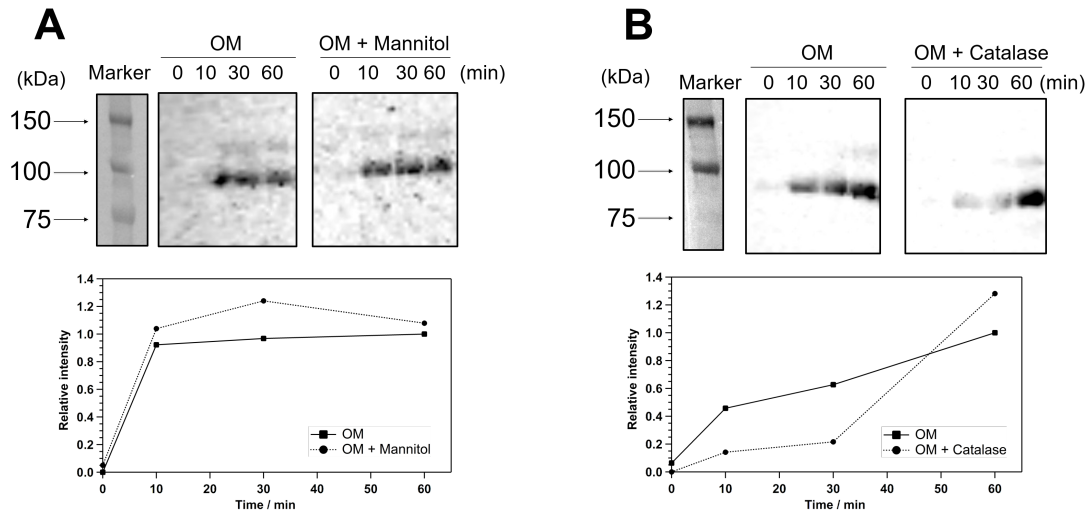

Figure 3.2 Oxyblot analysis of WT IRP2 in the presence of ROS scavengers

The time course of Oxyblot assay for oxidation in WT IRP2 with 20 mM mannitol (A), 1,000 units/ml catalase (B) under the OM conditions. A Western blot for oxidized IRP2 (upper panel) and time courses of the normalized intensity (lower panel) are shown.

3.3.2. Detection of H_2O_2 Production in the Oxidation Reaction of IRP2

To confirm the production of H_2O_2 during the oxidation of IRP2, we used a spectroscopic assay employing xylenol orange, by which the produced H_2O_2 can be quantified based on Fenton's reaction. In this assay, H_2O_2 oxidizes Fe^{2+} to form an Fe^{3+}-xylenol orange complex, which shows the characteristic absorbance at 595 nm (*9*). Addition of heme to IRP2 in the presence of DTT, the absorbance at 595 nm was increased (Fig. 3.3A, solid line), and the increase in the absorbance at 595 nm was suppressed in the presence of catalase (Fig. 3.3A, dashed line), demonstrating the production of H_2O_2 in the OM condition for IRP2. The produced H_2O_2 was quantified by the absorbance at 595 nm 15 min after addition of DTT (Fig. 3.3B). The concentration of H_2O_2 was 16.1 μM for IRP2. It should be noted here that IRP1 and IRP2ΔIDD, which showed no heme-induced oxidative modification, produced 13.3 μM and 16.9 μM of H_2O_2, respectively, comparable amount to that for IRP2 (Fig. 3.3B). Since WT IRP1 and IRP2ΔIDD could generate the similar amounts of H_2O_2 to that of WT IRP2, it is likely that the H_2O_2 produced from heme at HRM in the IDD domain is rapidly activated into more reactive species to oxidize the nearby amino acid residues, and the H_2O_2 produced from heme at HRM outside of the IDD domain is diffused to the solvent.

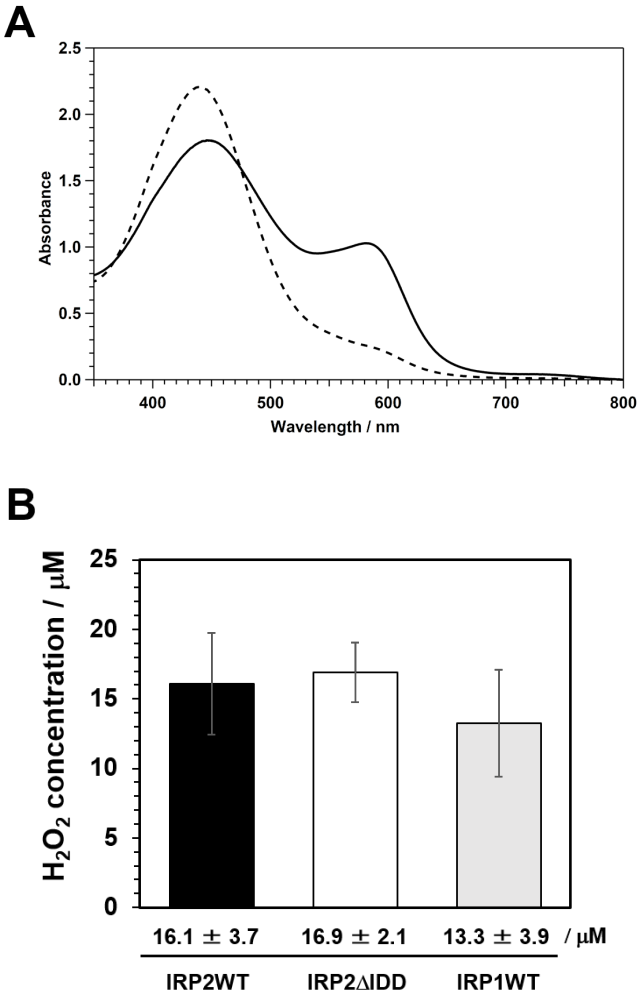

Figure 3.3 Spectroscopic assay for the H_2O_2 generation from heme-loaded IRPs
(A) Absorption spectra of reaction buffer containing 250 μM of ammonium ferrous sulfate, 125 μM of xylenol orange with heme-loaded IRPs and DTT in the absence (solid line) or presence (dashed line) of 4,000 units/ml catalase. At 15 min after the incubation of the mixture, the absorption spectra were measured and the amount of generated H_2O_2 was quantified by the absorbance at 595 nm. (B) H_2O_2 concentration generated from heme-loaded IRPs with DTT. The data points and error bars represent the means and standard deviations of three independent experiments using three different protein preparations

3.3.3. Metal-catalyzed Oxidation of IRP2 under OM Condition.

So far, I have investigated the heme-mediated oxidation of IRP2 and found the generation of H_2O_2 under the OM condition, which would be immediately consumed. In the oxidation process of Irr, the produced H_2O_2 induces the degradation of heme, leading to the release of iron from heme, which contributes to the metal-catalyzed oxidation of amino acid residues (*8*). To reveal the mechanism for the activation of H_2O_2 to more reactive species in IRP2, I investigated the H_2O_2-mediated degradation of heme in IRP2. To confirm the heme degradation, I measured UV-vis absorption spectra of WT IRP1, WT IRP2 and IRP2ΔIDD in the OM condition with 3-(2-Pyridyl)-5,6-diphenyl-1,2,4-triazine-*p,p*'-disulfonic acid monosodium salt hydrate (PDTS, also known as ferrozine), a specific chelator for iron showing the characteristic absorbance at 562 nm in the presence of ferrous iron (*10*). As illustrated in Fig. 3.4A-C, the absorbance at around 370 nm decreased concomitant with the increase at 562 nm for all IRPs in OM condition in the presence of PDTS. The decrease in the Soret band at around 370 nm derived from the characteristic heme bound to IRPs indicates heme degradation in this condition. In addition, the enhancement of absorbance at 562 nm obviously demonstrated the release of non-heme iron from the degraded heme bound to IRPs. The amount of produced non-heme iron were quantified by the absorption coefficient for PDTS-Fe^{2+} complex at 562 nm of 27.9 mM^{-1} cm^{-1} (*21*) (Fig. 3.4D). Unexpectedly, the production rate for non-heme iron from degraded heme for WT IRP2 were comparable to that of WT IRP1 and IRP2ΔIDD. These results revealed that heme at HRMs outside of the IDD domain rather than the heme bound to HRM in IDD domain is dominantly degraded, resulting in the production of non-heme iron, implying that the heme degradation by H_2O_2 is not the characteristic for heme-mediated oxidation in IRP2.

Additionally, the addition of iron chelator (EDTA), which suppresses the metal-catalyzed oxidation of proteins based on Fenton's reaction (*17*), did not suppress the oxidation of IRP2 (Fig. 3.5). This result suggested that the heme-mediated oxidation of IRP2 is not caused by the

non-heme iron-catalyzed manner as observed for Irr (*8*). Therefore, during the heme-mediated oxidation of IRP2, the generated H_2O_2 may be rapidly activated on the heme-iron into more reactive species which induce oxidation in IRP2, rather than the metal-catalyzed oxidation by non-heme iron released from heme.

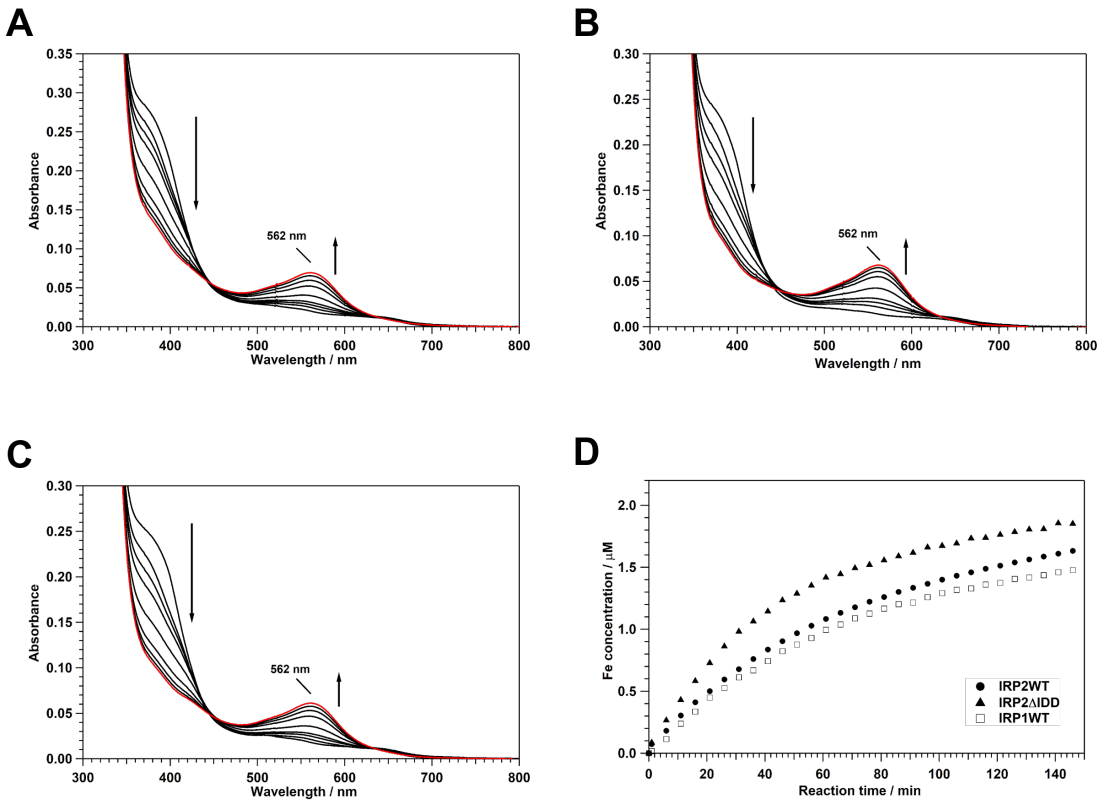

Figure 3.4 Absorption spectral changes in the OM condition of IRPs.
The absorption spectra of 5 μM of (A) WT IRP2, (B) IRP2ΔIDD and (C) WT IRP1 in OM condition in the presence of 100 μM of PDTS. The spectra were measured at 5 min intervals and the spectra for 0, 5, 10, 15, 30, 50, 90, 120, 150 min after the addition of DTT were displayed. (D) The concentration of iron are plotted against the reaction time. The concentration of produced iron are calculated based on the absorbance at 562 nm for each reaction time, which is derived from PDTS-Fe^{2+} complex, subtracting the initial absorbance at 562 nm (before the addition of DTT).

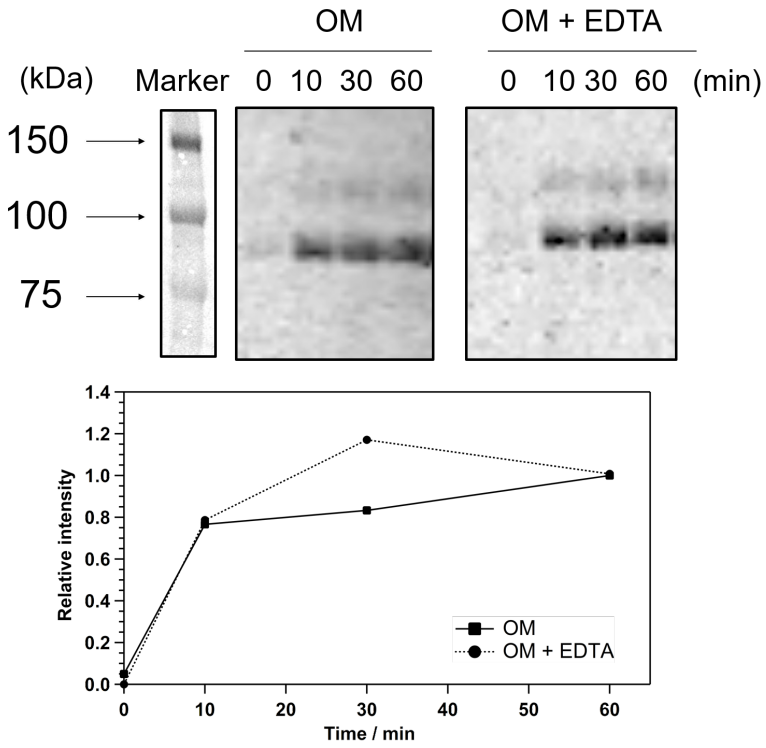

Figure 3.5 Oxyblot analysis of WT IRP2 in the presence or absence of EDTA

The time course of Oxyblot assay for oxidation in WT IRP2 with 1 mM of EDTA under the OM conditions. A western blot for oxidized IRP2 (upper panel) and a time course of the normalized intensity (lower panel) are shown.

3.4. Discussion

3.4.1. Heme-induced Oxidative Modification in IRP2

In this chapter III, to figure out the importance of heme binding to HRM in the IDD domain for the oxidative modification of IRP2, I conducted the *in vitro* Oxyblot assay for WT IRP1, WT IRP2 and IRP2ΔIDD in the OM condition. As previously suggested (*1, 3, 6*), I clearly demonstrated the *in vitro* heme-mediated oxidation in WT IRP2, but not WT IRP1 and IRP2ΔIDD (Fig. 3.1). Result from the addition of ROS scavenge, mannitol and catalase, showed that catalase suppressed the oxidation of IRP2, demonstrating the production of H_2O_2 during the oxidation of IRP2 (Fig. 3.2). The similar heme-mediated oxidation is also observed in Irr, bacterial transcription factor, via the heme binding to its HRM (*11, 12*). In the oxidation process for Irr, H_2O_2 is generated by the reduction of heme at first. Although the activation of molecular oxygen into H_2O_2 is a common reaction for typical hemoproteins such as myoglobin in the presence of reductant (*22*), no oxidation is observed in myoglobin under the OM condition, due to the insufficient reactivity of H_2O_2 to direct oxidation into the proteins (*8*). Indeed, in the oxidation of Irr, H_2O_2 generated from heme iron causes the degradation of heme and releases the non-heme iron, consequently H_2O_2 is converted into ·OH, which induces oxidative modification near the amino acid residues (*8*). Thus, I proposed that the H_2O_2 would be produced and activated into more reactive species in the heme-mediated oxidation of IRP2. Although the H_2O_2 production, heme degradation and release of non-heme iron were also observed for IRP2 in the OM condition, the rate of H_2O_2 production and non-heme iron release are comparable among WT IRP1, WT IRP2 and IRP2ΔIDD (Fig. 3.3 and 3.4), indicating that H_2O_2 may be generated dominantly from the heme at HRMs outside of the IDD domain, and the heme at HRM in IDD domain is not preferably degraded in the OM condition. These results proposed the different pathway for heme-mediated oxidation in IRP2 compared to Irr. As EDTA did not suppress the oxidation of IRP2 (Fig. 3.5), the non-heme iron would not

contribute to the oxidation in IRP2. Therefore, I speculated that H_2O_2 produced at HRM in the IDD domain may react with heme-iron to form more reactive species, instead of degradation of the heme.

3.4.2. Specificity of Oxidation in IRP2

As discussed above, while H_2O_2 and non-heme iron were detected from WT IRP1, WT IRP2 and IRP2ΔIDD under OM condition, only IRP2 suffered from heme-mediated oxidation. To understand this functional difference of heme among IRPs, I examined the heme environment for HRMs in IRPs. The heme binding environment in IRP1 and IRP2 was characterized in recent paper (*23*). In this paper, a heme intermediate specific to IRP2 was observed under reducing condition. Following the reduction of heme, only IRP2 showed the five-coordinate His-ligates heme. As it is previously reported that the heme ligand in IDD domain is replaced from Cys201 to His204 by reduction of heme, the ligand for this intermediate would be the His204 in IDD domain (*6*). Considering that the only IRP2 is oxidized by reduction of heme, the five-coordinate His-ligated heme would efficiently generate and activate ROS for IRP2 oxidation.

References.

1. K. Iwai, R. D. Klausner, T. A. Rouault, Requirements for iron-regulated degradation of the RNA binding protein, iron regulatory protein 2. *EMBO J* **14**, 5350-5357 (1995).
2. L. S. Goessling, D. P. Mascotti, R. E. Thach, Involvement of heme in the degradation of iron-regulatory protein 2. *J Biol Chem* **273**, 12555-12557 (1998).
3. K. Iwai *et al.*, Iron-dependent oxidation, ubiquitination, and degradation of iron regulatory protein 2: implications for degradation of oxidized proteins. *Proc Natl Acad Sci U S A* **95**, 4924-4928 (1998).
4. K. Yamanaka *et al.*, Identification of the ubiquitin-protein ligase that recognizes oxidized IRP2. *Nat Cell Biol* **5**, 336-340 (2003).
5. J. Jeong, T. A. Rouault, R. L. Levine, Identification of a heme-sensing domain in iron regulatory protein 2. *J Biol Chem* **279**, 45450-45454 (2004).
6. H. Ishikawa *et al.*, Involvement of heme regulatory motif in heme-mediated ubiquitination and degradation of IRP2. *Mol Cell* **19**, 171-181 (2005).
7. R. L. Levine, J. A. Williams, E. R. Stadtman, E. Shacter, Carbonyl assays for determination of oxidatively modified proteins. *Methods Enzymol* **233**, 346-357 (1994).
8. C. Kitatsuji *et al.*, Protein oxidation mediated by heme-induced active site conversion specific for heme-regulated transcription factor, iron response regulator. *Sci Rep* **6**, 18703 (2016).
9. Z. Y. Jiang, A. C. Woollard, S. P. Wolff, Hydrogen peroxide production during experimental protein glycation. *FEBS Lett* **268**, 69-71 (1990).
10. J. Im, J. Lee, F. E. Loffler, Interference of ferric ions with ferrous iron quantification using the ferrozine assay. *J Microbiol Methods* **95**, 366-367 (2013).
11. Z. H. Qi, I. Hamza, M. R. O'Brian, Heme is an effector molecule for iron-dependent degradation of the bacterial iron response regulator (Irr) protein. *P Natl Acad Sci USA* **96**, 13056-13061 (1999).
12. H. Ishikawa *et al.*, Unusual heme binding in the bacterial iron response regulator protein: spectral characterization of heme binding to the heme regulatory motif. *Biochemistry* **50**, 1016-1022 (2011).
13. N. Smirnoff, Q. J. Cumbes, Hydroxyl Radical Scavenging Activity of Compatible Solutes. *Phytochemistry* **28**, 1057-1060 (1989).
14. B. Shen, R. G. Jensen, H. J. Bohnert, Mannitol protects against oxidation by hydroxyl radicals. *Plant Physiol* **115**, 527-532 (1997).
15. J. A. Escobar, M. A. Rubio, E. A. Lissi, Sod and catalase inactivation by singlet oxygen and peroxyl radicals. *Free Radic Biol Med* **20**, 285-290 (1996).
16. M. M. Goyal, A. Basak, Hydroxyl radical generation theory: a possible explanation of unexplained actions of mammalian catalase. *Int J Biochem Mol Biol* **3**, 282-289 (2012).
17. E. R. Stadtman, Oxidation of free amino acids and amino acid residues in proteins by

radiolysis and by metal-catalyzed reactions. *Annu Rev Biochem* **62**, 797-821 (1993).

18. J. R. Requena, C. C. Chao, R. L. Levine, E. R. Stadtman, Glutamic and aminoadipic semialdehydes are the main carbonyl products of metal-catalyzed oxidation of proteins. *Proc Natl Acad Sci U S A* **98**, 69-74 (2001).
19. J. Mattana, L. Margiloff, P. C. Singhal, Metal-catalyzed oxidation of extracellular matrix proteins disrupts integrin-mediated adhesion of mesangial cells. *Biochem Biophys Res Commun* **233**, 50-55 (1997).
20. E. R. Stadtman, C. N. Oliver, Metal-catalyzed oxidation of proteins. Physiological consequences. *J Biol Chem* **266**, 2005-2008 (1991).
21. B. S. Berlett, R. L. Levine, P. B. Chock, M. Chevion, E. R. Stadtman, Antioxidant activity of Ferrozine-iron-amino acid complexes. *Proc Natl Acad Sci U S A* **98**, 451-456 (2001).
22. K. Shikama, Nature of the FeO2 bonding in myoglobin and hemoglobin: A new molecular paradigm. *Prog Biophys Mol Biol* **91**, 83-162 (2006).
23. M. Ogura *et al.*, Redox-dependent axial ligand replacement and its functional significance in heme-bound iron regulatory proteins. *J Inorg Biochem* **182**, 238-248 (2018).

CHAPTER IV

IDENTIFICATION OF OXIDATION SITE IN IRP2 AND INVESTIGATION OF THE MECHANISM FOR HEME-MEDIATED OXIDATION

ABSTRACT

In chapter II, I observed the heme-induced inhibition of IRPs-IRE complex formation. The heme bound to HRM near the IRE binding site sterically interferes the interaction of IRPs with IRE. On the other hand, the heme binding to HRM causes the larger impact on the inhibition of IRP2-IRE complex formation, and also induces the dissociation of IRP2 from IRE. Thus, I proved that the role of each HRM in IRPs would be different in the heme-induced regulation.

In chapter III, I found the *in vitro* heme-mediated oxidation in IRP2, but not WT IRP1 and IRP2ΔIDD, demonstrating that the IDD domain is required for the heme-mediated oxidation. As catalase suppressed the oxidation, H_2O_2 seems to be involved in the oxidation of IRP2. However, WT IRP1 and IRP2ΔIDD also produced the similar amounts of H_2O_2 compared to WT IRP2. Also the oxidation of IRP2 would not proceed via metal-catalyzed oxidation by non-heme iron. Therefore, I proposed that H_2O_2 produced in the heme at the HRM in the IDD domain may be activated into more reactive species, which oxidize the amino acids in IRP2.

In this chapter IV, I revealed the high valent iron (IV)-oxo complex formation in IRPs in the presence of heme and H_2O_2, suggesting that the production of ·OH on the heme at HRMs in IRPs as a result of the formation of the iron (IV)-oxo complex. In addition, I also identified the amino acid residues by ·OH in IRP2 by measuring the mass spectra. I detected one peptide oxidized in the presence of heme and reductant, DTT. Further MS/MS analysis of the peptide revealed that Met552 in the peptide was the oxidized amino acid residue in IRP2. The model structure of IRP2 suggested that Met552 is located close to the IDD domain, where ·OH would be generated, indicating that ·OH produced on the heme at HRM in the IDD domain could oxidize the Met552, which would be important for subsequent recognition by the ubiquitin ligase, HOIL-1, leading to the degradation of IRP2.

4.1. Introduction.

In chapter II, I demonstrated the heme-induced inhibition of IRPs-IRE complex formation. The heme bound to HRM near IRE binding site sterically inhibits the complex formation between IRPs and IRE. Importantly, the heme bound to HRM in the IDD domain causes larger impact on the inhibition, and even promotes the dissociation of IRP2 from IRE. These differences would be derived from the different heme binding environment and structural flexibility among the HRMs. In chapter III, I found the *in vitro* heme-mediated oxidation, which is characteristic reaction for IRP2. Although the production of H_2O_2 by reduction of heme iron in IRPs was observed, the heme-mediated oxidation for IRP2 seems not to be caused via metal catalyzed oxidation, which is reported in the heme-mediated oxidation of Irr (*2, 3*). Thus, it is indicated that the heme bound to HRM in the IDD domain produces H_2O_2, which would be immediately consumed for the further activation into more reactive species by reacting with heme-iron, instead of degrading the heme.

In this chapter IV, to fully understand the mechanism for heme-mediated oxidative modification in IRP2, I examined to observe the further activation of H_2O_2, which forms more reactive species, ·OH, by the heme in HRM in the IDD domain of IRP2. Further activation of H_2O_2 to ·OH through high valent heme reaction intermediates, iron (IV)-oxo complexes such as Compound I and Compound II, is a typical reaction of hemoproteins (*4, 5*). As all of IR1WT, WT IRP2 and IRP2ΔIDD formed the high valent iron (IV)-oxo complex in the presence of heme and H_2O_2 confirmed by using guaiacol as an oxidized substrate. Therefore, ·OH, which is produced as a result of the formation of the iron (IV)-oxo complex would oxidizes the amino acid residues in IRP2.

I further assessed the oxidation site in IRP2 in the OM condition. By carrying out the mass spectrometry measurements for intact and oxidized IRP2, a peptide consisting of Thr544-Ser568 in domain 3 of IRP2 was identified as the oxidized peptide in the OM

condition. The further MS/MS analysis of this peptide fragment showed that the mass of Met552 in the peptide was increased by 16 Da upon the oxidation reaction, revealing that Met552 is one of the oxidation site in IRP2. Given that model structure of IRP2 predicted the position of Met552 close to the IDD domain, the ·OH generated on the heme at the HRM in IDD domain could access to Met552, leading to the oxidation. Thus, the mechanism for heme-mediated oxidation at Met552 in IRP2 has been proposed.

4.2. Experimental Procedures.

4.2.1 Materials.

All chemicals were purchased from Wako Pure Chemical Industries (Osaka, Japan), Nacalai Tesque (Kyoto, Japan) or Sigma-Aldrich (St. Louis, MO, USA), and used without further purification.

4.2.2 Protein Expression and Purification

The procedure for the expression and purification of IRPs are described in Chapter II.

4.2.3 Peroxidase Assay of Heme-loaded IRPs in the Presence of H_2O_2.

The peroxidase activity of IRPs was monitored by using guaiacol as the reducing substrate in the presence of heme and H_2O_2. The oxidized product (tetraguaiacol) was measured by the absorbance at 470 nm using the extinction coefficient of 26.6 $mM^{-1}cm^{-1}$ (*1*).

Purified IRPs (1 μM) in 50 mM HEPES buffer were incubated with three equivalent amounts of hemin dissolved in DMF, followed by the removal of unbound heme through spin column as described above and 10 mM guaiacol in 30 % ethanol was added. The reaction was initiated by addition of 200 μM H_2O_2 and UV-vis absorption spectra were monitored at 20 °C with 3 min interval until 90 min.

4.2.4 Measurements of Mass Spectra for Oxidized IRP2 by Using MALDI TOF

<u>Preparation of samples for in-gel digestion</u>

The samples for the in-gel digestion were prepared as follow (*6*). All samples contained 5 μM purified IRP2 in the buffer of 50 mM Tris-HCl at pH 7.4. The samples for the oxidation reaction contained various reagent including 15 μM hemin, 2 mM DTT, 5 μM Iron II) Sulfate heptahydrate (KANTO CHEMICAL) solution and 2 mM DTT, or 2 mM H_2O_2 (Wako). The oxidation reactions were performed in 1.5 mL Eppendorf tube on ice and the reaction time were measured after addition of DTT or H_2O_2. At 15 minutes after the reaction start, 20 μL of each sample including intact IRP2 was added into 5 μL of 5 × loading buffer containing 60 mM Tris-HCl (pH 6.8), 25% glycerol, 2 % SDS, 14.4 mM 2-mercaptoethanol and 0.1% bromophenol blue. All samples were heated at a 100 °C for 5 minutes and applied to the wells of a 7.5 % polyacrylamide gel (Atto) with the molecular weight marker (APRO SCIENCE) for SDS-PAGE. The electrophoresis was performed at room temperature, 20 mA constant for approximately 60 minutes with the electrophoresis buffer composed of 25 mM Tris-HCl, 192 mM glycine at pH 8.8. After the electrophoresis, the gel was washed twice by ultrapure water for 5 minutes and stained by Coomassie Brilliant Blue using CBB Stain One (Nacalai Tesque) for 30 minutes. After the staining, the gel was washed by ultrapure water until appearing of the visible band with molecular weight corresponding to that of IRP2. Washed gel was followed by excising the bands detected at around 100 kDa on the gel into about 1 × 1 mm cubes by using surgical blade (FEATHER) in clean bench.

In-gel reduction, alkylation and destaining of IRP2

Each gel pieces was destained by addition of 200 μL destaining solution containing 50 % acetonitrile and 25 mM ammonium hydrogen carbonate with shaking at 200 rpm at room temperature for 30 minutes. After removing the destaining solution, 100 μL acetonitrile were added to the gel pieces and shaken for 10 minutes and gel pieces shrank by removing the acetonitrile. The shrunk gel pieces were evaporated by centrifuging at 2,600 rpm with vacuum

(MV-100, TOMY). The 100 μL of reducing solution composed of 10 mM DTT and 25 mM ammonium hydrogen carbonate were added to the dry gel pieces and incubated at a 56 °C water bath for 45 minutes. The solution was removed 45 minutes later and washed by 100 μL washing solution with 25 mM ammonium hydrogen carbonate for 10 minutes with shaking. Removing the solution was followed by the addition of 100 μL alkylation solution containing 1 % iodoacetamide and 25 mM ammonium hydrogen carbonate and incubation with shaking at room temperature in dark for 45 minutes. The solution were removed, and washing and destaining were performed by addition of 100 μL washing solution and 100 μL destaining solution. The gel pieces were dried again by addition of 200 μL acetonitrile and centrifuging with vacuum as above.

In-gel digestion by trypsin

The dried gel pieces were dissolved by the 20 μL trypsin solution containing 50 mM ammonium hydrogen carbonate, 12 ng/μL trypsin (Sequencing Modified Trypsin, Promega), and 0.01 % ProteaseMax™ surfactant, Trypsin Enhancer (Promega) for 10 minutes on ice. This step was followed by addition of the 30 μL efficient digestion solution composed of 50 mM ammonium hydrogen carbonate and 0.01 % ProteaseMax™ surfactant, Trypsin Enhancer and incubation at 56 °C in a water bath for 1 hour. The full length IRP2 was cleaved at the carboxyl side (C-terminal side) of Lys or Arg by trypsin to produce peptides fragments and the yielded peptides were efficiently extracted from the gel into solution by trypsin enhancer through this step. The solution was centrifuged at 15,000 g for 10 seconds and supernatants were transferred into the new tubes. The trypsin were inactivated by adding the 0.5 % TFA.

Preparation of samples for MALDI-TOF measurement

Zip tip C_{18} was used for concentration, purification and desalting of the sample for the MALDI-TOF measurement. The resin of zip tip was equilibrated with the 10 μL 0.1 % TFA solution three times and absorbed the peptide in sample solutions via 10 times pipetting. The peptides-loaded resin was washed with 10 μL 0.1 % TFA solution three times. The peptides were eluted with 1.5 μL 0.1 % TFA solution, which contains 50 % acetonitrile and is saturated with the α-Cyano-4-hydroxycinnamic acid (CHCA) matrix. The eluted peptide samples were putted onto the metal plate for measurement.

Procedure for MALDI-TOF and MALDI-TOF-TOF measurement

The metal plate with dried peptide sample was inserted into autoflex™ speed (Bruker) for MALDI-TOF measurement. The matrix associated samples were ionized by the pulse irradiation of 337 nm nitrogen laser and TOF measurement was used for detecting the mass-to-charge ratio of ionized peptides. All MALDI-TOF measurements were performed in the positive reflector mode and mass spectra were added up to 1,000 laser shots. The obtained spectra were smoothed and calibrated using Data Explorer (Applied Biosystems).

To identify the oxidized amino acid residue in IRP2, I used TOF/TOF™ 5800 system (AB SCIEX). The ionization of peptides fragments was followed by the selection of precursor ion via QuantTis™ precursor Ion Selector and fragmentation with air in the collision induced dissociation (CID) cell. The MS/MS spectra were obtained by measuring the mass-to-charge ratio of each fragment. The web server MASCOT MS/MS Ions Search (MATRIX SCIENCE) was used to analyze the obtained MS/MS spectra for assigning the peaks to calculated mass of the fragments derived from IRP2 in Swiss Prot database.

4.3. Results

4.3.1. Peroxidase Activity Assay for IRPs in the presence of H2O2

From the results in chapter III, I suggested that the further activation of H_2O_2 to more reactive species, ·OH, by the heme in HRM of the IDD domain of IRP2. Such further activation of H_2O_2 to ·OH through high valent heme reaction intermediates, iron (IV)-oxo complexes such as Compound I and Compound II, is a typical reaction of hemoproteins (*4, 5*). To confirm the formation of these iron (IV)-oxo complexes at the heme binding to HRMs in IRPs, we monitored the peroxidase activity of heme-bound IRPs by using *o*-methoxyphenol (guaiacol) as the reducing substrate, as previously reported (*7, 8*). The iron(IV)-oxo complexes oxidize guaiacol to form oligomeric products (tetraguaiacol), which is detected by the specific absorbance at 470 nm with the extinction coefficient of 26.6 $mM^{-1}cm^{-1}$ (*1*). The addition of H_2O_2 to ferric heme-bound IRP2 in the presence of excess amount of guaiacol resulted in the increase in the absorbance at 470 nm, showing the formation of iron (IV)-oxo complexes oxidizing guaiacol to tetraguaiacol (Fig. 4.1A).

Although IRP1 and IRP2ΔIDD did not show the heme-induced oxidative modification, guaiacol was oxidized by both IRP1 and IRP2ΔIDD (Fig. 4.1B), indicating the possibility of the ·OH production in heme at HRM outside of the IDD domain. The oxidation of guaiacol was observed for myoglobin, but no oxidative modification was detected and the radical transfer to the aromatic residues on the protein surface was reported (*9-12*). The radical center at the amino acid residue on the protein surface would be quenched by the buffer solution or form an intermolecular covalent bond to form dimeric protein (*13, 14*). In IRP1 and IRP2ΔIDD, ·OH would also oxidize amino acid residues to form a radical center, which would be transferred to the surface of the protein to be quenched without the oxidative modification of amino acid residues.

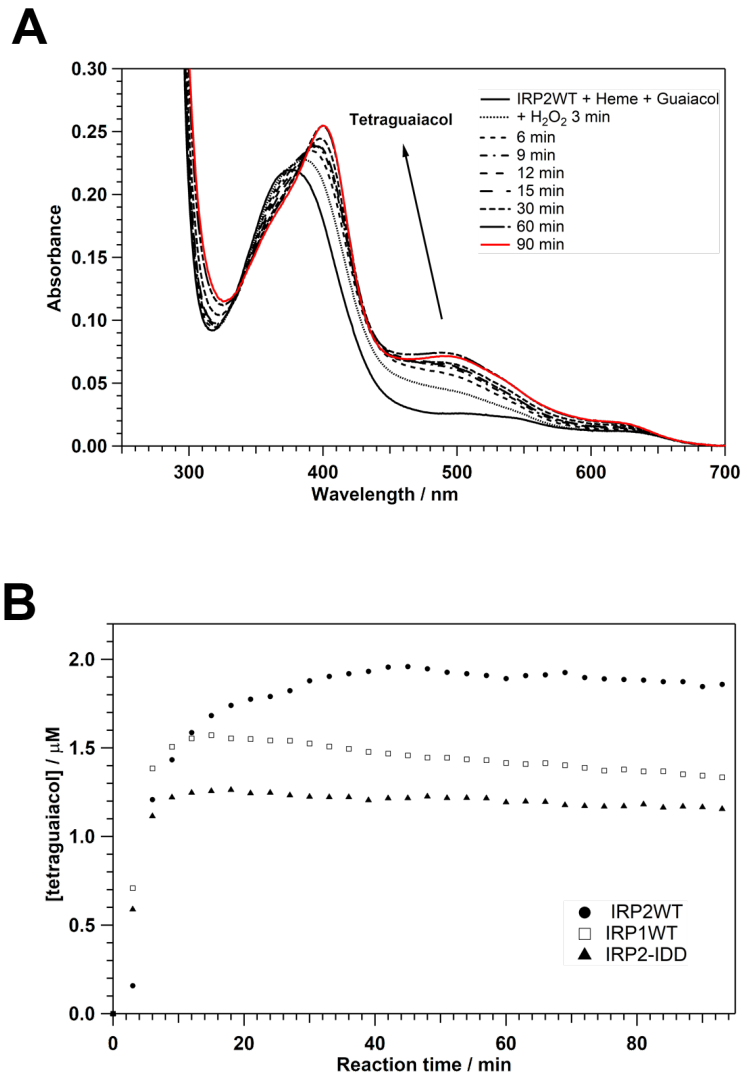

Figure 4.1 Peroxidase activity for IRPs in the presence of heme and H_2O_2

Tetraguaiacol production from heme-loaded IRPs with guaiacol in the presence of H_2O_2. (A) Spectral changes were monitored during heme-IRPs reaction with H_2O_2 in the presence of guaiacol at 3 min intervals. Tetraguaiacol production was confirmed by the increase of absorbance at 470 nm and its concentration was calculated by using molar absorption coefficient (ε_{470} = 26.6 $mM^{-1}cm^{-1}$) (*1*). (B) The concentrations of tetraguaiacol generated by the oxidation reaction from heme-loaded IRPs with H_2O_2 were plotted against reaction time.

4.3.2. Identification of Heme-mediated Oxidation Peptides in IRP2

To fully understand the mechanism of heme-mediated oxidation in IRP2, I tried to identify the oxidation site in IRP2 in the OM condition. To determine the oxidation sites in IRP2, I conducted the MALDI-TOF mass spectrometry. After intact or oxidized IRP2 is digested by trypsin into various peptide fragments, the mass spectra for these peptides were obtained (Fig. 4.2).

As previously indicated, the addition of heme and DTT with IRP2 would generate ·OH, and since the mixing of iron salt and reductant such as DTT with oxygen can produce H_2O_2 and ·OH (*15-17*), this condition was used for the typical condition for the production of ·OH independent from heme. Fig. 4.2 illustrated the obtained mass spectra of intact IRP2 (Fig. 4.2A), or IRP2 under various reaction conditions: IRP2 treated with heme and DTT for 15 minutes (Fig. 4.2B) or 40 minutes (Fig. 4.2C), with iron salt and DTT for 15 minutes (Fig. 4.2D) or with excess amount of H_2O_2 for 15 minutes (Fig. 4.2E). By comparing these spectra, the mass shift accompanied by the oxidation is shown in the area between m/z 2550-2600 (Fig. 4.3). In this region, two mass peaks at m/z 2568.3 and m/z 2584.3 are observed. From the amino acid sequence of IRP2, the mass peak at m/z 2568.3 is assigned to the peptide fragment consisting of amino acids Thr544-Ser568 (calculated monoisotopic mass is 2568.3 Da), and peak at m/z 2584.3 corresponds to the oxidized peptide fragment with insertion of one oxygen atom (atomic mass is 15.9994 amu) to Thr544-Ser568 fragment. Although the relative intensity of mass peak at m/z 2584.3 is very small in intact IRP2 (Fig. 4.3A), in IRP2 with heme and DTT the intensity significantly increased proportional to the reaction time (Fig. 4.3B and C). Furthermore, the increase of this peak intensity is also detected by treatment with iron salt and DTT (Fig. 4.3D), but not with H_2O_2 (Fig. 4.3E) corresponding to the result of Oxyblot analysis, in which H_2O_2 did not induce oxidative modification in IRP2 (Fig. 3.1A). These mass spectra shown in Fig. 4.2 and 4.3 suggest the oxidation of an amino acid residue within Thr544-Ser568 fragment by

·OH generated by treatment of heme and DTT rather than by H_2O_2.

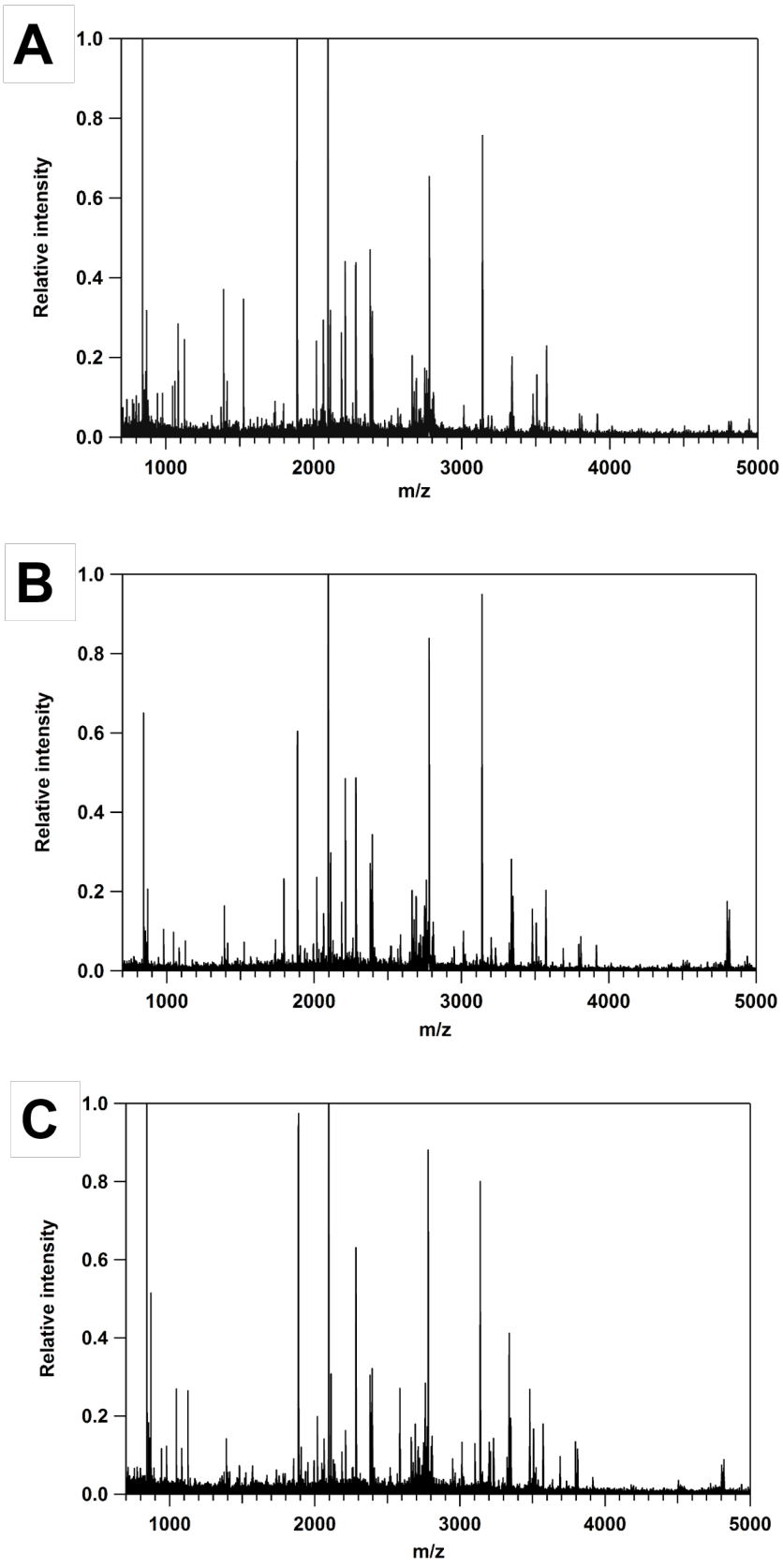

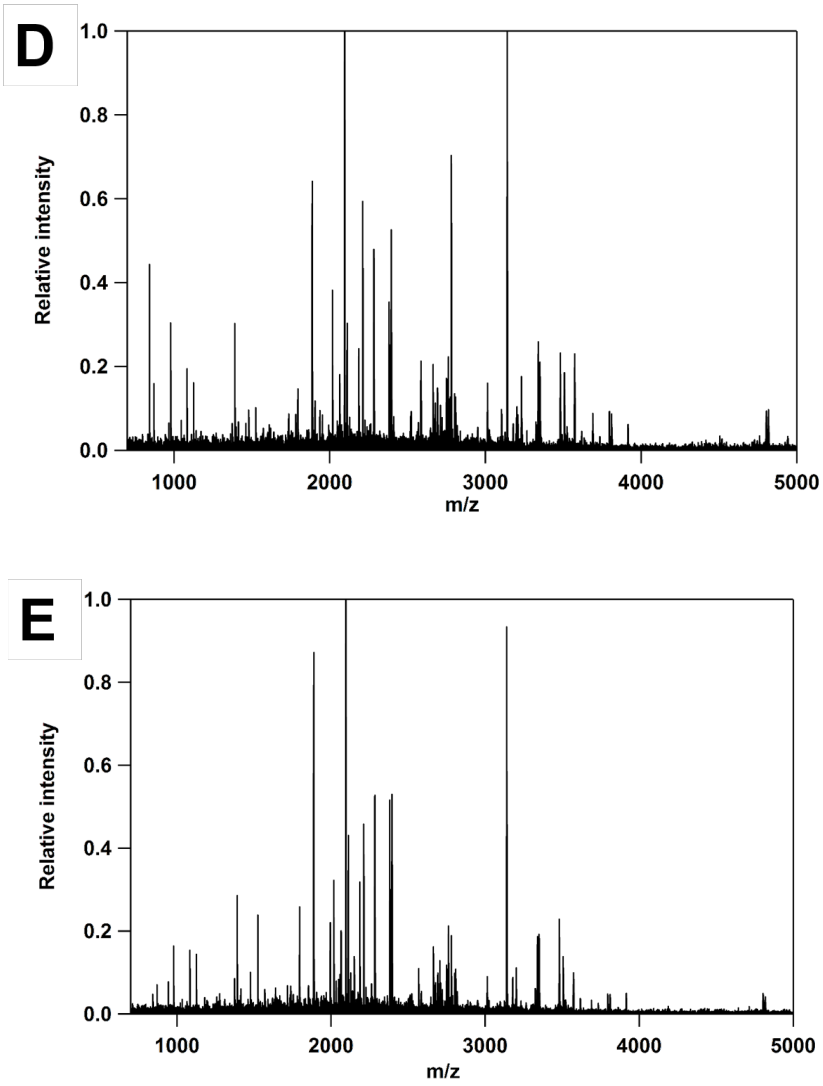

Figure 4.2. Mass spectra of intact and oxidized IRP2

Mass spectra of IRP2 with no treatment (A), heme and DTT for 15 minutes (B) or 40 minutes (C), iron salt and DTT for 15 minutes (D), and H_2O_2 for 15 minutes (E), respectively. The horizontal axis shows the mass-to-charge ratio, and vertical axis shows the relative intensity of fragment ions normalized to the intensity of the peak at m/z 2096 which is the highest intense peak.

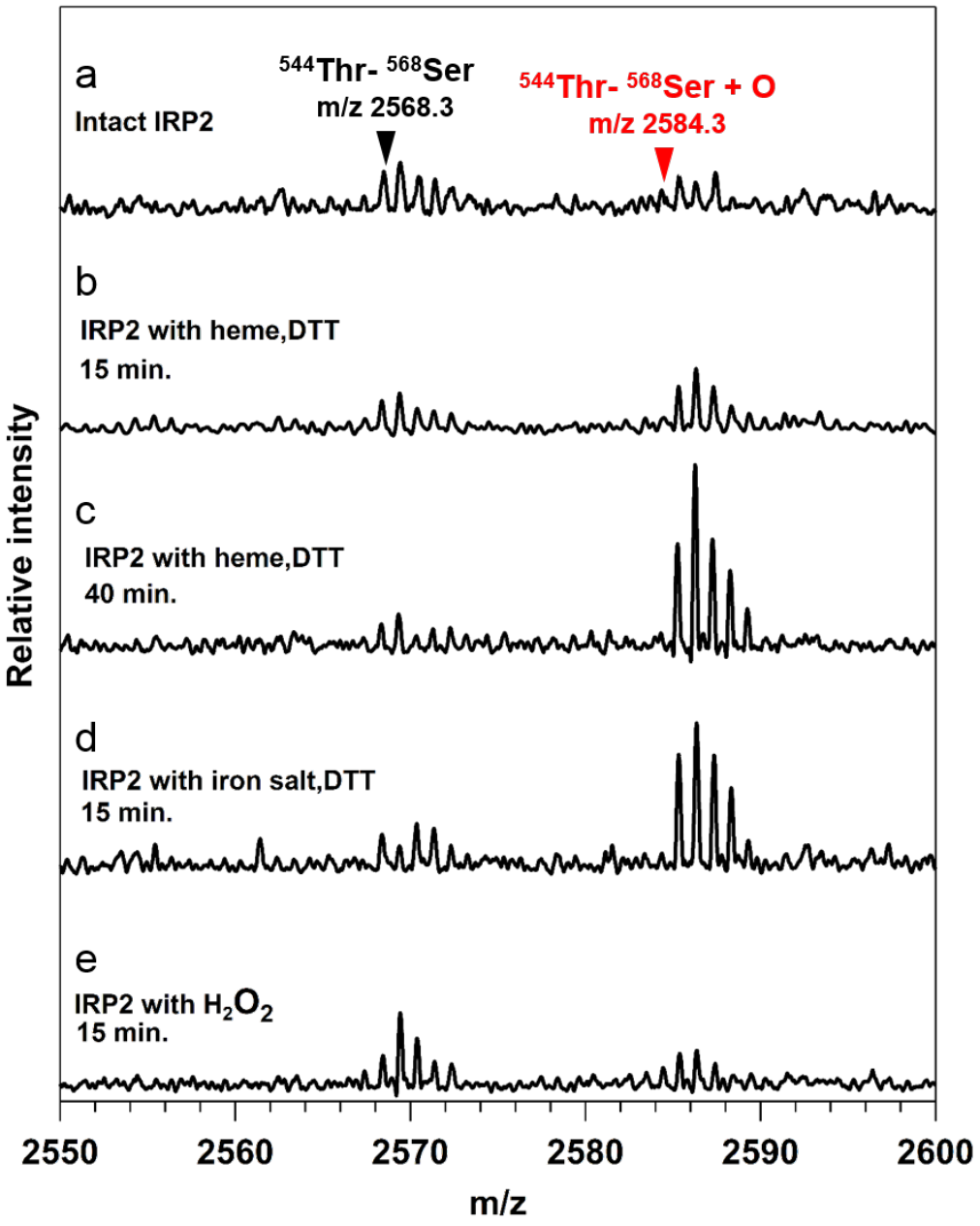

Figure 4.3. Mass spectra between at m/z 2550-2600

Mass spectra from m/z 2550 to m/z 2600 of the IRP2 with no treatment (a), heme and DTT for 15 minutes (b) or 40 minutes (c), iron salt and DTT for 15 minutes (d), and H_2O_2 for 15 minutes (e), respectively. The intense peak at m.z 2584.3 was detected in the spectra of IRP2 treated with heme and DTT, or iron salt and DTT.

4.3.3. Identification of Oxidized Amino Acid Residue in IRP2

To further determine the oxidized amino acid residue in Thr544-Ser568 of IRP2, I carried out the MALDI-TOF/TOF mass spectrometry and analyzed the TOF/TOF spectra for the peak at m/z 2584.3 in mass spectra of IRP2 treated with heme and DTT for 40 minutes. As shown in Fig. 4.4, I found that the mass of the residues between Val553 and Lys568 (y6 – y16 fragment in Fig. 4.4) have not changed after the oxidation. On the other hand, the mass of the residues between Met552 and Gly553 is increased by 16 Da. As methionine is more sensitive to oxidation than glycine (*18*), I identified Met552 as the oxidation site in IRP2. Regarding the product of Met552 oxidation, it is known that the reaction of Met with ROS such as ·OH produces a methionine sulfoxide (+16 Da from native methionine, Fig. 4.5) (*19*). Therefore, I proved that Met552 is oxidized by ·OH, producing the methionine sulfoxide.

As oxidized IRP2 is a substrate for HOIL-1 (*17*), I supposed that the oxidation at Met552 plays an important role in recognition by HOIL1. One possibility for the effect of Met552 oxidation to recognition by HOIL-1 is some conformational changes in IRP2 because the oxidation of methionine to methionine sulfoxide can trigger some conformational changes (*20-22*), including secondary structure in the protein. Therefore, we examined whether the oxidation at Met552 also affect the secondary structure in IRP2.

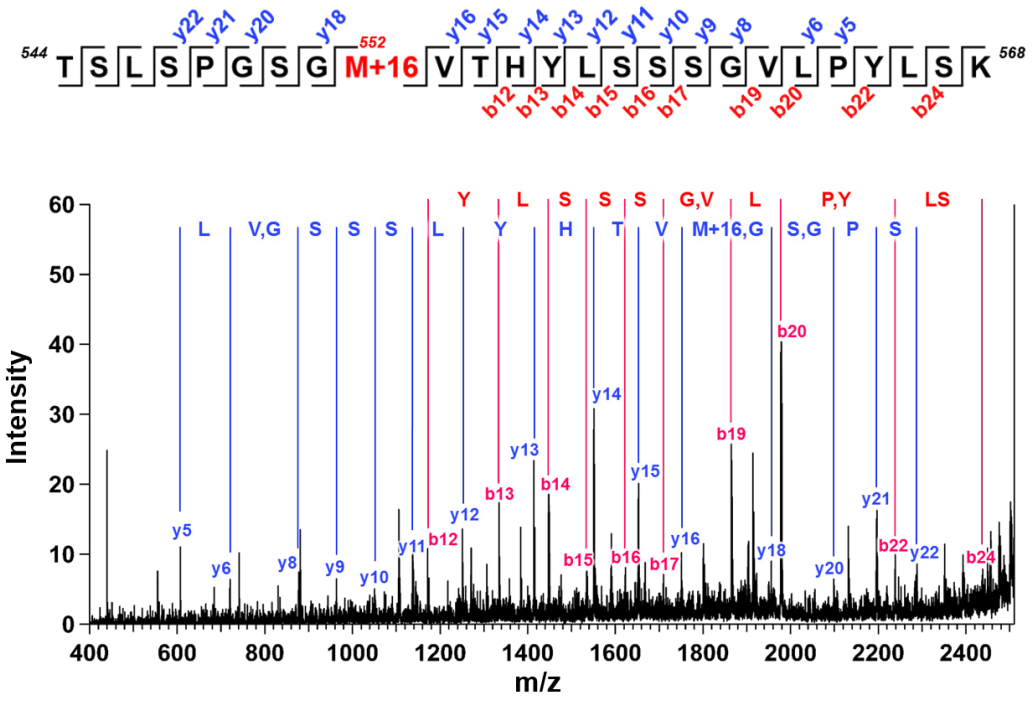

Figure 4.4. MS/MS spectrum of the peptide fragments detected at m/z 2584.3 in oxidized IRP2

We selected the peak at m/z 2584 in the mass spectrum of IRP2 treated with heme and DTT for 40 min as the precursor ion for the MS/MS fragmentation. Blue lines show the fragment peaks derived from *y*-ion and red lines are derived from *b*-ion of the peptide consisting of amino acids ^{544}Thr - ^{568}Ser, shown above.

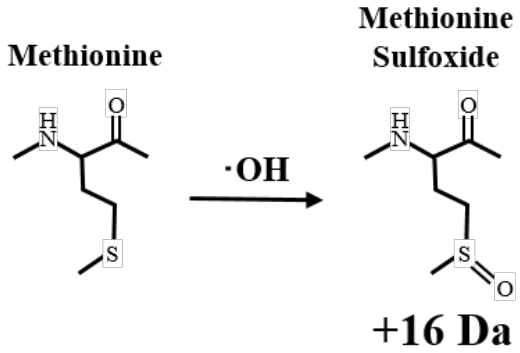

Figure 4.5. Methionine oxidation by ·OH

Reaction of methionine with ·OH produces the methionine sulfoxide, and the mass increase by 16 Da.

4.4. Discussion

4.4.1. Mechanism of Heme-mediated ROS generation and Oxidation in IRP2

In chapter III, it was suggested that generated H_2O_2 is activated by heme-iron without degrading heme during the heme-mediated oxidation of IRP2. In this chapter, I observed the formation of iron (IV)-oxo complex such as Compound I and Compound II in IRP2 in the presence of heme and H_2O_2, confirmed by the oxidation of guaiacol, whereas the WT IRP1 and IRP2ΔIDD also showed the oxidation of guaiacol with the lower rate of production compared to WT IRP2 (Fig. 4.1). As a result of the formation of iron (IV)-oxo complex, the O–O bond derived from H_2O_2 is cleaved heterorytically to form Compound I or homolytically to form Compound II (*5*). Compound I is a generally unstable transient intermediate and in most heme peroxidases it is stabilized by the designed structure around heme such as distal histidine and tryptophan or proximal asparagine (*4, 23, 24*). As IRPs have not been found as peroxidase, these amino acid residues would not compose in IRPs and heme in IRPs could rather form Compound II. The homolytical cleavage of O–O bond results in the release of ·OH (*25*), suggesting the formation of Compound II in the reaction of H_2O_2 with heme at HRMs, leading to the generation of ·OH. Although the generation of product in the peroxidase assay from IRP2 was slightly more efficient, IRP1 can also generate oxidized guaiacol (Fig. 7), implying the possibility of the generation of ·OH in heme at HRM in IRP1 or HRM outside of the IDD domain. The radical produced at the heme moiety of myoglobin is transferred to protein surface through the aromatic residue, which does not induce oxidation in myoglobin (*9-12*). Thus, the ·OH produced in heme at HRM outside of the IDD domain may also be transferred to the surface of protein, resulting in the quench of the radical by buffer and no induction of oxidation in protein.

On the other hand, the ·OH generated on the heme at HRM in IDD domain would cause the oxidative modification in amino acid residues in IRP2. I in turn tried to identify the oxidation site in IRP2 by the ·OH generated on the heme at HRM in the IDD domain. The intact and oxidized IRP2 digested into peptide fragments by trypsin were used for the mass spectrometry to detect the oxidized residues (Fig. 4.2 and 4.3). Unexpectedly, I did not detect any modified peptide derived from the IDD domain, where the heme would generate the ·OH. The mass spectra of IRP2 in the OM condition instead showed the oxidized peptide fragment consisting of Thr544-Ser568 in domain 3 of IRP2 (Fig. 4.3). Moreover, the MS/MS spectra of this oxidized peptide fragment revealed that Met552 in this peptide is oxidized with increase of 16 Da of its mass (Fig. 4.4), which corresponds to the methionine sulfoxide (Fig. 4.5). Considering the short life time of ·OH (*26*), it should react with the amino acid residue close to site where it was generated, indicating that this Met552 should be close to the heme at HRM in the IDD domain. To confirm location of Met552, I performed the homology modeling of IRP2 based on the crystal structure of IRP1 by using Swiss-Model (*27*), because the any structures of IRP2 have not been reported. The model structure is shown in Fig. 4.6A. In this structure, the IDD domain is represented in an oblong shape image, because the sequence of IDD is not conserved either in its homologue IRP1 or other proteins, and so there is the lack of the structural information for IDD domain. Fig. 4.6B shows that Met552 is located in the close proximity to IDD domain. Combined with the intrinsic structural flexibility of IDD domain (Fig. 2.5B), it is suggested that the ·OH generated at the HRM in the IDD domain might be able to access to Met552 to induce its oxidation.

I could not exclude the possibility that the ·OH-induced oxidation occur at other than the Met552, particularly at the amino acids in IDD domain, which is responsible for the heme-mediated oxidation. However, this Met552 is not conserved in IRP1 at the corresponding site (Fig. 1.5), indicating that the existence of Met552 may be one of the specific property of IRP2 for the heme-mediated oxidation.

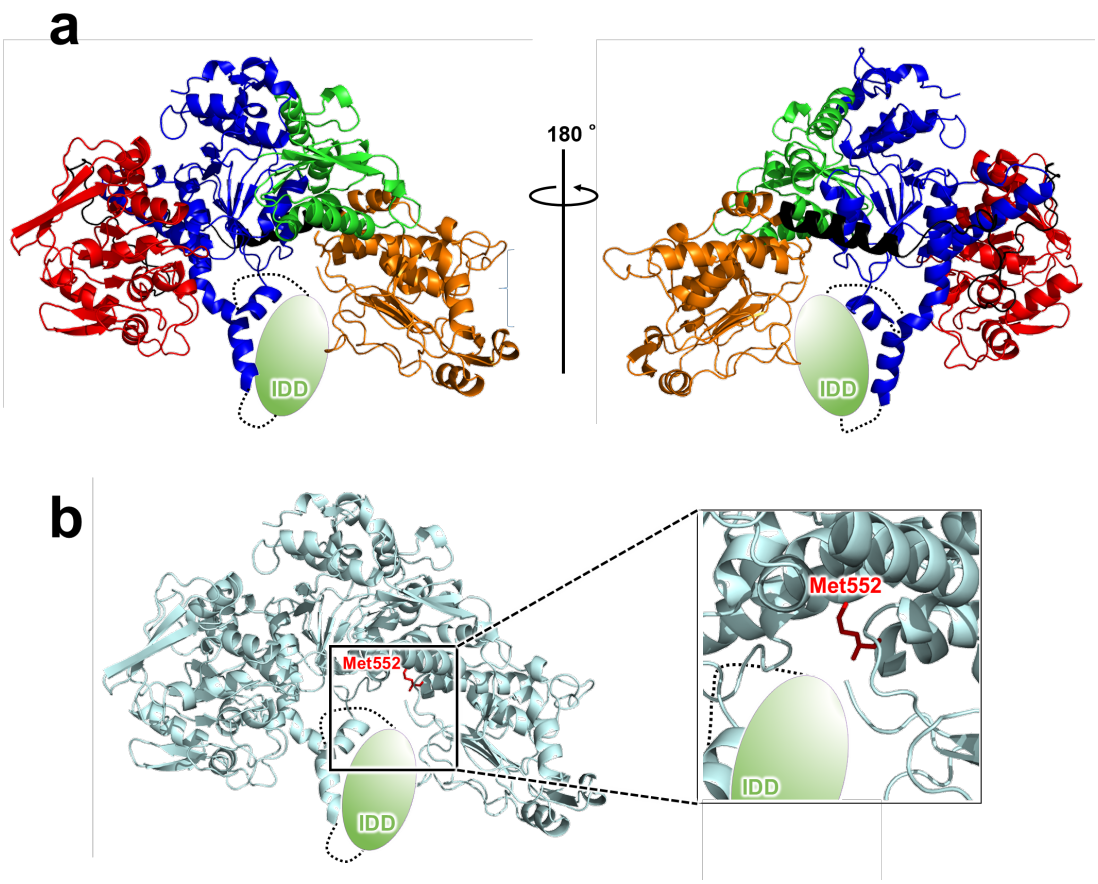

Figure 4.6. Model structure of IRP2 and the location of IDD and ^{552}Met

(a) This model structure was obtained by using SWISS-MODEL (URL:http://swissmodel.expasy.org/) based on the crystal structure of IRP1 with Ft IRE (PDB ID : 3SNP) as the template. IDD is represented as a light green oblong. The domain colors correspond to those of IRP1 in Figure 6. (b) Enlarged view of the region including IDD domain and ^{552}Met.

References

1. B. Chance, A. C. Maehly, Assay of Catalases and Peroxidases. *Method Enzymol* **2**, 764-775 (1955).
2. H. Ishikawa *et al.*, Unusual heme binding in the bacterial iron response regulator protein: spectral characterization of heme binding to the heme regulatory motif. *Biochemistry* **50**, 1016-1022 (2011).
3. C. Kitatsuji *et al.*, Protein oxidation mediated by heme-induced active site conversion specific for heme-regulated transcription factor, iron response regulator. *Sci Rep* **6**, 18703 (2016).
4. P. C. E. Moody, E. L. Raven, The Nature and Reactivity of Ferryl Heme in Compounds I and II. *Acc Chem Res* **51**, 427-435 (2018).
5. X. Huang, J. T. Groves, Oxygen Activation and Radical Transformations in Heme Proteins and Metalloporphyrins. *Chem Rev* **118**, 2491-2553 (2018).
6. A. Shevchenko, H. Tomas, J. Havlis, J. V. Olsen, M. Mann, In-gel digestion for mass spectrometric characterization of proteins and proteomes. *Nat Protoc* **1**, 2856-2860 (2006).
7. C. S. Caruso, E. Biazin, F. A. Carvalho, M. Tabak, J. F. Bachega, Metals content of Glossoscolex paulistus extracellular hemoglobin: Its peroxidase activity and the importance of these ions in the protein stability. *J Inorg Biochem* **161**, 63-72 (2016).
8. T. Uchida, M. Sasaki, Y. Tanaka, K. Ishimori, A Dye-Decolorizing Peroxidase from Vibrio cholerae. *Biochemistry* **54**, 6610-6621 (2015).
9. T. Hayashi *et al.*, Peroxidase activity of myoglobin is enhanced by chemical mutation of heme-propionates. *J Am Chem Soc* **121**, 7747-7750 (1999).
10. C. Giulivi, E. Cadenas, Heme protein radicals: formation, fate, and biological consequences. *Free Radic Biol Med* **24**, 269-279 (1998).
11. H. Ostdal, L. H. Skibsted, H. J. Andersen, Formation of long-lived protein radicals in the reaction between H2O2-activated metmyoglobin and other proteins. *Free Radic Biol Med* **23**, 754-761 (1997).
12. P. R. Ortiz de Montellano, C. E. Catalano, Epoxidation of styrene by hemoglobin and myoglobin. Transfer of oxidizing equivalents to the protein surface. *J Biol Chem* **260**, 9265-9271 (1985).
13. D. Tew, P. R. Ortiz de Montellano, The myoglobin protein radical. Coupling of Tyr-103 to Tyr-151 in the H2O2-mediated cross-linking of sperm whale myoglobin. *J Biol Chem* **263**, 17880-17886 (1988).
14. P. K. Witting, D. J. Douglas, A. G. Mauk, Reaction of human myoglobin and H2O2. Involvement of a thiyl radical produced at cysteine 110. *J Biol Chem* **275**, 20391-20398 (2000).
15. E. R. Stadtman, C. N. Oliver, Metal-catalyzed oxidation of proteins. Physiological

consequences. *J Biol Chem* **266**, 2005-2008 (1991).

16. K. Iwai *et al.*, Iron-dependent oxidation, ubiquitination, and degradation of iron regulatory protein 2: implications for degradation of oxidized proteins. *Proc Natl Acad Sci U S A* **95**, 4924-4928 (1998).
17. K. Yamanaka *et al.*, Identification of the ubiquitin-protein ligase that recognizes oxidized IRP2. *Nat Cell Biol* **5**, 336-340 (2003).
18. G. Xu, M. R. Chance, Hydroxyl radical-mediated modification of proteins as probes for structural proteomics. *Chem Rev* **107**, 3514-3543 (2007).
19. W. Vogt, Oxidation of methionyl residues in proteins: tools, targets, and reversal. *Free Radic Biol Med* **18**, 93-105 (1995).
20. G. M. Anantharamaiah *et al.*, Effect of oxidation on the properties of apolipoproteins A-I and A-II. *J Lipid Res* **29**, 309-318 (1988).
21. H. L. Schenck, G. P. Dado, S. H. Gellman, Redox-triggered secondary structure changes in the aggregated states of a designed methionine-rich peptide. *J Am Chem Soc* **118**, 12487-12494 (1996).
22. J. E. Zull, S. K. Smith, R. Wiltshire, Effect of methionine oxidation and deletion of amino-terminal residues on the conformation of parathyroid hormone. Circular dichroism studies. *J Biol Chem* **265**, 5671-5676 (1990).
23. M. Wirstam, M. R. A. Blomberg, P. E. M. Siegbahn, Reaction mechanism of compound I formation in heme peroxidases: A density functional theory study. *J Am Chem Soc* **121**, 10178-10185 (1999).
24. A. Gumiero, C. L. Metcalfe, A. R. Pearson, E. L. Raven, P. C. Moody, Nature of the ferryl heme in compounds I and II. *J Biol Chem* **286**, 1260-1268 (2011).
25. T. L. Poulos, Heme enzyme structure and function. *Chem Rev* **114**, 3919-3962 (2014).
26. P. Attri *et al.*, Generation mechanism of hydroxyl radical species and its lifetime prediction during the plasma-initiated ultraviolet (UV) photolysis. *Sci Rep* **5**, 9332 (2015).
27. M. Biasini *et al.*, SWISS-MODEL: modelling protein tertiary and quaternary structure using evolutionary information. *Nucleic Acids Res* **42**, W252-258 (2014).

CHAPTER V

GENERAL CONCLUSIONS

Iron homeostasis is tightly maintained in mammalian cells by IRPs. Recent study showed that HRMs conserved between IRP1 and IRP2 could specifically bind to heme, but only IRP2 has been known to be regulated by heme binding to HRM in its unique IDD domain. In this thesis, I focused on the functional roles of heme binding to IRPs, including the heme-induced regulation of IRPs-IRE complex formation and heme-mediated oxidation of IRP2.

Heme-induced Regulation of Complex Formation between IRPs and IRE (Chapter II)

In chapter II, I clearly revealed that the heme binding to HRMs in IRPs affects the complex formation with IRE. Although the heme bound to HRM near the IRE binding site in IRPs sterically inhibits the complex formation of IRPs with IRE, the heme binding to HRM in the IDD domain of IRP2 exhibits more significant effects on the inhibition and even promotes the dissociation of IRP2 from IRE. Thus, I revealed that the association of both IRPs and IRE is regulated by heme binding to HRMs, whereas the heme-induced dissociation of IRP2 via heme binding to HRM in IDD domain functionally differentiates IRP2 from IRP1.

Detection of Heme-mediated Oxidation of IRP2 and Identification of The ROS (Chapter III)

The heme-mediated degradation of IRP2, in which the heme binding to IDD domain would trigger the oxidation of IRP2, has already been suggested. In chapter III, I demonstrated that *in vitro* heme-mediated oxidation takes place in WT IRP2, but not in WT IRP1 or IRP2ΔIDD, revealing that the oxidation of IRP2 is required the heme binding to IDD domain. The addition of catalase suppressed the oxidation, indicating the involvement and generation of H_2O_2 in the heme-mediated oxidation in IRP2. As the reactivity of H_2O_2 is not enough to directly oxidize

amino acids in IRP2, the H_2O_2 is supposed to be activated into more reactive species to induce oxidation in IRP2. In the oxidation of IRP2, the activation of H_2O_2 would not be catalyzed by non-heme iron, which was observed in the oxidation of Irr. Therefore, it has been proposed that the produced H_2O_2 in the heme at HRM in IDD domain might be activated by reacting with heme-iron, resulting in the generation of more reactive species such as ·OH.

Identification of Oxidation Site in IRP2 and Investigation of the Mechanism for Heme-mediated Oxidation (Chapter IV)

In chapter IV, I revealed the high valent iron (IV)-oxo complex formation in IRPs in the presence of heme and H_2O_2, suggesting that the production of ·OH on the heme at HRMs in IRPs as a result of the formation of the iron (IV)-oxo complex. Thus, ·OH produced on the heme at HRM in IDD domain would take part in the oxidation of IRP2, as proposed in chapter III. I also tried to identify the oxidation site in IRP2. The mass spectra of oxidized IRP2 showed that the peptide derived from domain 3 is oxidized in the OM condition. Further MS/MS analysis clarified the oxidation of Met552 in the peptide. As Met552 seems to be close to the IDD domain in model structure of IRP2, the ·OH produced on the heme at HRM in IDD domain may be able to access to Met552 to oxidize the amino acid residue.

The Functional Role of Heme Binding to HRMs in IRPs

Throughout this thesis, I revealed that heme acts as a signaling molecule to alter the function of both IRPs including the regulation of IRPs-IRE complex and triggering the oxidative modification in IRP2, via its binding to HRMs in IRPs. From the present study, it is suggested that the heme binding to HRM in IDD domain of IRP2 causes the more drastic effect on the inhibition of the complex formation with IRE, compared to the heme binding to HRMs

in IRP1. Regarding the affinity of heme to the HRMs in IRPs, the heme dissociation constant for isolated IDD domain was estimated to be 90 nM , whereas the dissociation constant for Cys mutant of recombinant IRP1 (IRP1/C118 and IRP1/C300A, respectively) were determined to be 740 nM and 800 nM, respectively. From these results, the affinity of heme to HRM in the IDD domain of IRP2 seems to be around 9-fold higher than that for HRMs in IRP1 or HRMs outside of the IDD domain in IRP2, suggesting that heme preferentially bind to HRM in the IDD domain under low heme concentrations in cells. Given the low concentration of cytosolic labile heme, which is considered to be less than 1 μM (*1, 2*) and estimated at around 20-40 nM in most cases (*3*), heme would be able to reversibly bind to HRM in IDD domain of IRP2 in steady state cells, whereas the HRMs in IRP1 or HRMs outside of the IDD domain could bind to heme when the heme level gets higher. Therefore, the HRM in IDD domain of IRP2 is more sensitive to the changes of cytosolic labile heme level, and the higher concentration of free heme induces the inhibition of IRP1-IRE complex formation.

The Physiological Importance of Heme-mediated Regulation of IRPs

The present study in this thesis demonstrated that ferric heme causes inhibition of complex formation of IRPs with IRE. On the other hand, the heme-mediated oxidation in IRP2 requires reductants and oxygen to produces ROS. Although the valence of heme buffered or transported intracellular condition is unknown, ferrous heme is generally cytotoxic because of its reactivity with molecular oxygen to generate ROS (*4, 5*). The regulation of IRPs-IRE complex formation by the binding of ferric heme is reasonable in order to avoid the ROS generation by ferrous heme around the mRNA, which may cause diseases as found in the Alzheimer' disease patients (*6*). Therefore, the ferric heme-induced inhibition of IRPs-IRE complex should be prior to the reducing the heme, which triggers the oxidation of IRP2. Given the reducing environment in cytosol (*7*), heme must be in a reduced form if it exists as 'free heme', indicating that IRPs may

bind to ferric heme transported by unknown transporter, in which the heme is kept as a ferric state to avoid the cytotoxicity.

References

1. S. Sassa, Biological implications of heme metabolism. *J Clin Biochem Nutr* **38**, 138-155 (2006).
2. X. Yuan *et al.*, Regulation of intracellular heme trafficking revealed by subcellular reporters. *Proc Natl Acad Sci U S A* **113**, E5144-5152 (2016).
3. D. A. Hanna *et al.*, Heme dynamics and trafficking factors revealed by genetically encoded fluorescent heme sensors. *Proc Natl Acad Sci U S A* **113**, 7539-7544 (2016).
4. V. Jeney *et al.*, Pro-oxidant and cytotoxic effects of circulating heme. *Blood* **100**, 879-887 (2002).
5. F. A. D. T. G. Wagener *et al.*, Heme is a potent inducer of inflammation in mice and is counteracted by heme oxygenase. *Blood* **98**, 1802-1811 (2001).
6. M. A. Smith, P. L. R. Harris, L. M. Sayre, J. S. Beckman, G. Perry, Widespread peroxynitrite-mediated damage in Alzheimer's disease. *J Neurosci* **17**, 2653-2657 (1997).
7. J. J. Hu, L. X. Dong, C. E. Outten, The Redox Environment in the Mitochondrial Intermembrane Space Is Maintained Separately from the Cytosol and Matrix. *Journal of Biological Chemistry* **283**, 29126-29134 (2008).